



CHALMERS
UNIVERSITY OF TECHNOLOGY

Heat and Mass Transfer Modelling in a porous structure
Effect of body's heat and moisture loss on the microclimate of a hygiene product

Master's thesis in Innovative and Sustainable Chemical Engineering

DIVYA SURESH

MASTER'S THESIS 2016

**Heat and Mass Transfer Modelling
in a porous structure
Effect of body's heat and moisture loss on the
microclimate of a hygiene product**

DIVYA SURESH



CHALMERS
UNIVERSITY OF TECHNOLOGY

Department of Chemistry and Chemical Engineering
Division of Chemical Engineering
CHALMERS UNIVERSITY OF TECHNOLOGY
Gothenburg, Sweden 2016

Heat and Mass Transfer Modelling in a porous structure
Effect of body's heat and moisture loss on the microclimate of a hygiene product
DIVYA SURESH

© DIVYA SURESH, 2016.

Supervisor: Charlotta Hanson, Per Bergström
Examiner: Anders Rasmuson

Master's Thesis 2016
Department of Chemistry and Chemical Engineering
Division of Chemical Engineering
Chalmers University of Technology
SE-412 96 Gothenburg
Telephone +46 76 099 3937

Heat and Mass Transfer Modelling in a porous structure
Effect of body's heat and moisture loss on the microclimate of a hygiene product
DIVYA SURESH
Department of Chemistry and Chemical Engineering
Chalmers University of Technology

Abstract

The master thesis is aimed at visualizing the effect of body's heat and mass losses on the microclimate of a hygiene product. The microclimate is defined by the air layer between the body and the product. An acceptable model for the skin is aimed to be found through in depth literature study and is validated to be used in the next step. Following which, a model with the skin, air layer, porous domain and a microporous film is built with the aim of the investigating the transport processes from the skin towards the porous domain. This is built and analysed with the help of COMSOL Multiphysics. Using virtual tools for building model and analysing the results saves time and can be used as an aid to examine in depth the underlying concepts of the phenomena involved. The model is made as versatile as possible so as to be flexible to be used for other similar products. The major goal of the built model is to analyse the heat and mass transfer behavior, including condensation phenomenon as well.

In the model, advection and convection are found to be of lesser importance with the help of manual calculations and dimensionless numbers. Coupled heat and mass transfer is analysed in the working model highlighting the effect of radiation and condensation. Radiation has pronounced effect in the heat transfer thereby having the necessity to include it in the model. Condensation is incorporated in the model to see the effect with the heat and mass transfer profiles. To get a working model for condensation, additional terms are added pertaining to the description of condensation mechanism.

Varying the ambient and skin conditions in the model gives an idea regarding the temperature and concentration profiles as well as the details about condensation happening in the system. The model parameters such as the porous domain thickness, air layer thickness, porosity of the porous domain and breathability of the film are then varied to check for the difference in heat and mass transfer behavior. The trend for the percentage of moisture condensed for each of the parameters is obtained by the post analysis of the multiple simulations of varying parameter values.

Keywords: Condensation, Porous medium, Film, Air Layer, Heat and Mass transfer, COMSOL, skin

Acknowledgements

The Master thesis has been done at SCA Hygiene Products AB, Gothenburg.

Firstly, I would like to convey special thanks to Charlotta Hanson for giving me the opportunity to perform my thesis at SCA. I would like to thank my supervisors, Charlotta Hanson and Per Bergström for supervising me in this project with valuable inputs. I would also like to thank my examiner Anders Rasmuson for providing me guidance and comments throughout the project. Thanks to Bjorn Bragée from the COMSOL support team for helping me with the software related queries. Thanks to Shabira Abbas and Maria Sköld for allotting some time for me when I had questions regarding the skin. Lastly, but not to forget, I would like to convey my thanks for my family and friends for having been a constant pillar of support with positive energy all through my masters education at Chalmers.

Divya Suresh, Gothenburg, June 2016

Contents

1	Introduction	1
1.1	Goals	2
2	Background	3
2.1	SCA	3
3	Product	5
3.1	Overview	5
3.2	Absorbent core	6
3.3	Back sheet	6
4	Skin	9
4.1	Structure and function	9
4.2	Sweating and Transepidermal water loss	9
5	Transport Processes	11
5.1	Momentum transport	11
5.1.1	Fluid phase	11
5.1.2	Porous media	11
5.2	Heat Transport	12
5.2.1	Fluid phase	12
5.2.2	Porous medium	13
5.3	Mass transport	15
5.3.1	Fluid phase	15
5.3.2	Porous media	16
5.4	Evaporation and Condensation	17
6	Dimensionless numbers	19
6.1	Reynolds number	19
6.2	Nusselt number	19
6.3	Rayleigh number	20
6.4	Stark/Stefan number	20
6.5	Hottel number	20
6.6	Peclet number	21
7	Computational tool	23

8	Skin Model	25
9	Complete Model	27
9.1	Model Geometry	27
9.2	Model Assumptions	28
9.3	Model Data	29
9.4	Meshing and Solvers	29
9.5	Physics and Boundary Conditions	29
9.5.1	Momentum Transport	29
9.5.2	Heat Transport	30
9.5.3	Mass Transport	32
9.5.4	Condensation	34
10	Post Analysis	37
10.1	Skin as a boundary	37
10.2	Heat Transport	38
10.3	Mass Transport	40
10.4	Effect of Radiation	42
10.5	Effect of Condensation	44
10.5.1	Varying ambient and skin parameters	44
10.5.2	Significance of Condensation	50
10.5.3	Effect of evaporated water(EW)	53
10.5.4	Effect of Condensation rate	53
10.5.5	Thickness of porous domain	55
10.5.6	Thickness of the air layer	56
10.5.7	Porosity of the porous domain	57
10.5.8	Breathability of the film	58
11	Conclusion	59
11.1	Skin Model	59
11.2	Heat and Mass Transport	59
11.3	Condensation	60
12	Future Research	63
	Bibliography	65
A	Appendix	I
A.1	Calculations	I
A.2	Boundary Conditions	III
B	Appendix	V
B.1	Results	V

1

Introduction

Mathematical modelling of heat and mass transport in the porous media have been a boom in the field of research for several years to observe the fundamental transport phenomena. This research has broad range of engineering applications in industries such as textile, drying, paper and pulp, building materials, etc. [1]. The study in the project can be related to the researches in the textile industry focussed with comfort modelling, wherein hygiene product is substituted for clothing. The microclimate in a hygiene product(diaper) is an important consideration for the wearer of the product. Microclimate is defined as the air layer layer between the skin and the product and is dependent on the body of the wearer, the construction of the product and the heat and mass transfer that takes place in the system. Models for the analysis of the heat and mass transfer processes in the microclimate are thereby of primary importance in the development of new, efficient and comfortable products.

Several studies have been conducted in the textile industry where the transport processes in the microclimate are investigated [2]. One such modelling study has been performed by Wang et al. who focussed on the heat transfer properties within the textiles but the moisture losses from the human body is ignored [2]. Transfer of moisture has been accounted by Onofrei et al. In their model, heat and mass transfer is analysed in an uncoupled fashion [3]. An improvement to the above models has been proposed by Lotens et al. who included condensation of moisture as an additional physical phenomena in their study [4]. Since condensation plays an important role in the human body comfort and the product design, this project focusses on the investigation of transport processes based on the model proposed by Lotens et al. with modifications pertaining to the specific scope of modelling of the processes in a hygiene product.

In general, modelling is accomplished with the aid of computational power as otherwise, the laws governing these physical process would be complex to solve manually. Experimentally, it would be difficult to handle large volumes of data since there are several factors to be considered in the product design [5]. Computational modelling provides space for such detailed analysis, and is therefore used in these cases of product optimization.

1.1 Goals

The major goals of this study are:

- To find a simple and acceptable model for the skin.
- To construct a model for coupled heat and moisture transport away from the body through the hygiene product to the environment with the help of a computational tool. Also, in such a skin-product model, it is necessary to eliminate a few transport processes to obtain a simplified model so as to reduce the computational time.
- To investigate the condensation behaviour within the skin-product model

Analysis of these skin-product models are of vital importance to give a detailed understanding of the transport mechanisms, thereby contributing to the development of innovative and comfortable hygiene products.

A small portion of the hygiene product attached to the crotch part of the naked body, as highlighted in the Figure 1.1.1, is selected in this study to analyse the transport processes in that portion. This simple model could then be used as a base model for modelling the transport processes in a more complex product design.

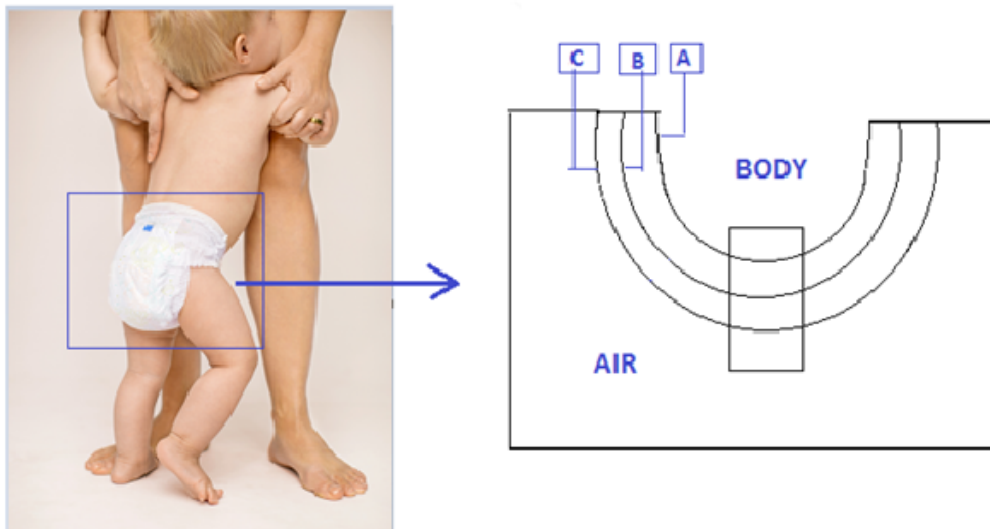


Figure 1.1.1:

Left Figure: Standing naked baby wearing the product;

Right Figure: Simple product model where A → skin, B → product's inner boundary, C → product's outer boundary, A-B → air layer between skin and product, B-C → product core

2

Background

2.1 SCA

Svenska Cellulose Aktiebolaget(SCA) is Europe's largest forest owner, which makes the company offer a considerable attention towards the sustainable forest management. It is one of the the leading global hygiene products and forest products group. SCA has been initiated in 1929 and is responsible for production of sustainable personal care, tissue and forest products. In over 100 countries, the sales have been established through strong product brands. In 2015, the sales has aggregated up to 115 billion SEK[6].

The personal care business sector at SCA is known for three types of products - baby care products, female hygiene products and adult incontinence products. The sales for all the three types are worldwide. The major SCA brands under which the products are sold include Libero,Libresse, Nosotras, Saba and TENA. In the year of 2014 in Europe, SCA market positions stand first for incontinence products, followed by baby care and the feminine care products [7].

2. Background

3

Product

3.1 Overview

Among the hygiene products, as mentioned earlier, there are three major groups of products - baby care, feminine hygiene and adult incontinence. These are grouped to belong to the same category of absorbent products, but varies in the amount and characteristics of the liquid absorbed onto the product [8, 7]. This study is primarily focussed on the research of the baby care products but the results could be used as a basis for other hygiene products as well.



Figure 3.1.1: Schematic representation of a modern diaper [9]

Though the product is offered in several styles with varying consumer features, the basic elements in the diaper construction remains the same. Diaper fluid handling could be visualized as four zones [10, 11]

- Top sheet, being the layer closest to the skin, allows liquid to quickly pass through the layers underneath.
- Acquisition layer, between the top sheet and the core, helps in uniform liquid

distribution within the core [10, 11].

- Absorbent core consists of a blend of polyacrylate superabsorber (SAP) and fluff cellulose pulp fibres. The pulp fibres offer integrity to the absorbent core. The core is responsible for absorption of the liquid and locks it within the SAP polymeric structure so that the liquid does not come in contact with the skin even under pressure.
- Back sheet, the outer layer of the product, is composed of a polyolefin with or without the presence of filler particles in it. It is water-resistant and safeguards the liquid from leaking to the outer [10, 11].

In the study, only two major components are taken into consideration to substitute the diaper - absorbent core and the back sheet.

3.2 Absorbent core

The absorbent core weighs up to 80% of the diaper weight, and hence it is an important material to discuss. The pulp fibres within the core are vital for the distribution of the liquid and they are also needed for the liquid absorption and retention. To be able to offer those functions, a porous network with a defined capillary structure is required [12].

The porous medium is generally categorised by the properties such as porosity, permeability and tensile strength [13]. Also the macroscopic properties of the medium are predicted by the microscopic pore structure models [14]. Due to condensation, swelling and deformations of the porous structure result followed with a varied porosity of the porous medium. But the structural changes due to condensation is not of specific interest in this study.

3.3 Back sheet

Conventionally, the back sheet of the product has been non breathable, which has appeared to show skin discomfort. This has led to the finding and use of breathable microporous outer film. Microporous film has the benefits of curtailing the skin from excess hydration, thereby diminishing the skin rashes [15].

The breathable microporous outer film consists of several micro pores and the pores are connected. The film is liquid impermeable but allows steam and perspiration to penetrate. Breathability is usually measured by the moisture vapour transmission rate through the film [16].

The film has been found to be best composed of polyolefin and inorganic filler particles. The polyolefin could be polyethylene, polypropylene or copolymer of both,

whereas the inorganic filler particles could be calcium carbonate, barium sulphate or other finely powdered inorganic particles [16]. Most commonly the film is made of polyethylene and calcium carbonate filler, which is demonstrated in Figure 3.3.1. This polymer-filler mixture is extruded as a 'non-porous film'. Then it is stretched mechanically to form the film which has high pore-to-pore connections so as to allow the air and moisture penetration through the film layer [16]. There has been many researches going on to find a suitable cost effective breathable film.

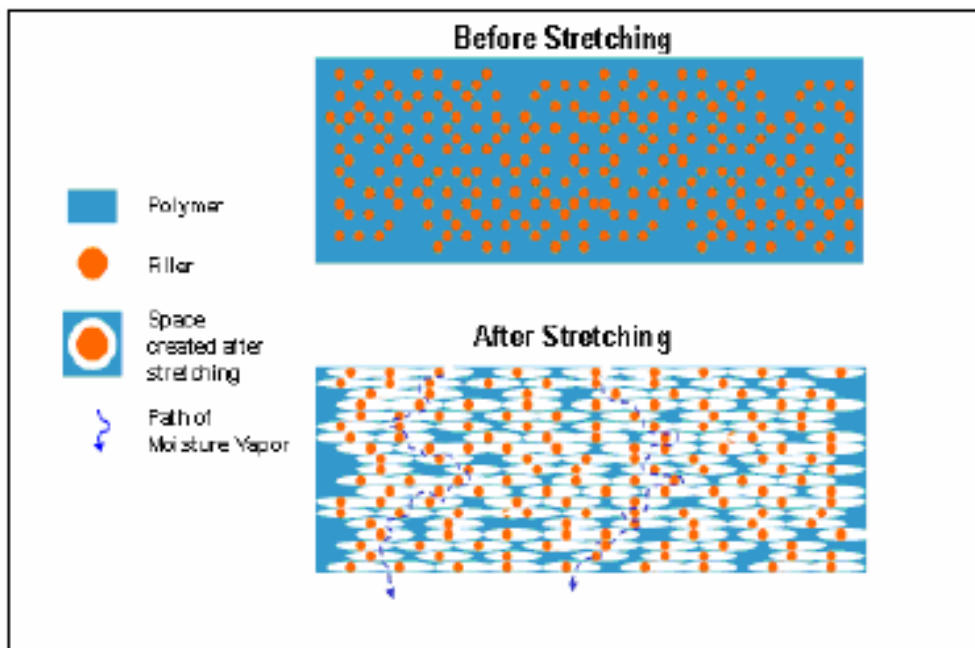


Figure 3.3.1: Polymer-filler microporous film

3. Product

4

Skin

4.1 Structure and function

Skin has several functions, but its primary function is to serve as a protection barrier for the body from the environment. This behaviour drives it to regulate the inward and outward movement of water molecules, electrolytes and other substances. Also the barrier offers strong protection against microorganisms, ultraviolet radiation and other toxic agents [17].

Viewing skin anatomically, it is divided into epidermis, dermis and hypodermis layers. Epidermis, the outermost layer serves as a physical and chemical barrier to the environment. The main cells in this layer are keratinocytes, which synthesize the protein keratin. Epidermis is composed of four layers, separately formed by the differing stages of keratinocyte maturation. Out of which, the most important is the topmost stratum corneum layer, which comprises the final outcome of the keratinocyte maturation. Epidermis has to retain sufficient water quantity in order to keep the stratum corneum hydrated so as to maintain the flexibility and deformability of the layer. Next structural layer of the skin is the dermis, which is responsible for giving support to the skin. Beneath dermis is the hypodermis layer which is known to store fats [17].

The stratum corneum contains substances to attract and hold water, known as natural moisturizing factor (NMF). NMF absorbs moisture from the outer environment and the deep skin layers, thus would make the outermost skin layer to stay hydrated irrespective of the drying feature of the outer environment. This balance is crucial for maintaining the skin elasticity and flexibility, also to perform its main barrier function. The outcome of the disruption of the balance is the skin hydration or skin dryness, resulting in other skin problems [18].

4.2 Sweating and Transepidermal water loss

The water loss from the viable tissues of the skin to the outer environment can pass the skin layer either by active transport (sweating) or by passive diffusion (transepidermal water loss) [19]. Sweating is a mechanism from the sweat glands to regulate the body

temperature, that is, when the body is excessively heated, sweat is produced and is evaporated to result in cooling of the body [20]. It may express psychological stress as well. Transepidermal water loss (TEWL) refers to water loss from the skin's stratum corneum layer, which also includes the water loss due to expired water vapour. It is not visible to the naked eye and it is not produced on demand for thermal regulation by the sweat glands. If the skin temperature is below 30°C and if the external environment temperature is below 20°C , there is no thermal sweat gland activity seen, provided there should be no forced convection or heat produced from the body (through exercise) [21]. In this study, sweating and TEWL are not differentiated, and are jointly considered as moisture loss from the body. The study deals only with the vapour phase, which helps in concluding that moisture loss from the body can be assumed as evaporated water (EW). EW is visualised as either TEWL or both TEWL and evaporated sweat.

5

Transport Processes

Transport processes within the microclimate, product and the surrounding environment govern the comfort of the product. Thus, this section will give an overview of various heat, mass and momentum transport processes within the fluid phase and porous material. Heat transfer occurs through conduction, flow, convection and radiation. Mass transfer occurs through diffusion, flow and convection. These transport processes in addition to evaporation and condensation are studied.

5.1 Momentum transport

5.1.1 Fluid phase

Fluid flow is generally demonstrated with the help of Navier-Stokes equation [22], shown below. The assumption of incompressible fluid flow is considered.

$$\rho\left(\frac{\partial \vec{v}}{\partial t} + v \cdot \nabla \vec{v}\right) = \mu \nabla^2 \vec{v} + \nabla P + g_i \quad (5.1.1)$$

Where v , μ , P , ρ represents the velocity, viscosity, pressure and density of the fluid respectively. The left hand side of the equation denotes the inertial forces. The first, second and the third term on the right hand side of the equation denotes the viscous forces, pressure forces and other external forces acting on the fluid, respectively [23].

5.1.2 Porous media

Flow in this study is assumed laminar because the vapour flow rate in realistic case models may not be too high for the flow to be turbulent. The laminar fluid flow in the porous media can be expressed by Darcy's law, shown in the Equation 5.1.2,

$$\bar{u}_g = -\frac{k_g}{\mu_g}(\nabla P_g - \rho_g \bar{g}) \quad (5.1.2)$$

where u_g is the darcy's velocity, k_g is the permeability, and μ_g is the viscosity of the fluid phase. This equation is valid when the boundary shear is ignored [24]. Bound-

ary shear is ignored because the fibre structure is porous and the fibres themselves are assumed non porous [25].

5.2 Heat Transport

5.2.1 Fluid phase

Conduction and Flow

Heat transfer by conduction and flow in pure fluids is described by the following equation.

$$\rho c_p \frac{\partial T}{\partial t} + \rho c_p \mathbf{v} \cdot \nabla T = \nabla \cdot (k \nabla T) + \dot{q} \quad (5.2.1)$$

Where \dot{q} represents the heat production per unit volume [26].

Heat transfer by conduction is usually achieved through molecular interaction. The molecules of faster motion being at a higher energy level transfers energy to the nearby molecules which are at a lower energy level. This occurs if there is a temperature gradient within the system and also molecules of solid, liquid or gas are to be present. The first term on the left side of the Equation 5.2.1 refers to the accumulation of energy. The first term on the right side of the Equation 5.2.1 is the net rate of heat conduction into a unit volume. k is the thermal conductivity of the material and ∇T is the temperature gradient. This is commonly called the Fourier's law of heat conduction and states that the heat transfer rate is proportional to the temperature gradient. The negative sign of the term indicates that the heat flow is in the direction of negative temperature gradient (∇T) [27].

The second term on the left side of the Equation 5.2.1 denotes transfer of energy due to the fluid flow [26]. ρ is the density, c_p is the specific heat at constant pressure, \mathbf{v} is the velocity, ∇T is given by $(T - T_{ref})$, T_{ref} refers to the reference temperature. Heat transfer by flow is due to the bulk transport of fluid. [26].

Convection

Heat Transfer by convection refers to movement of heat from one surface to an adjacent fluid where the bulk fluid motion is important. It is the means of energy transfer between surface and the adjacent fluid. In engineering, the convection heat transfer rate is expressed as,

$$\frac{q}{A} = h \Delta T \quad (5.2.2)$$

where h is the convective heat transfer coefficient, q/A is the heat flux, and ΔT is the temperature difference [27].

Depending on the driving forces, bulk fluid flow could be laminar or turbulent. There are two categories of convection - free or natural convection and forced convection. Natural convection is due the buoyance force caused by the density differences which

exist due the temperature variations, whereas the driving force for the forced convection is produced by an external means such as a fan or a pump [24]. Furthermore, natural convection could be classified as external and internal natural convection. The former defines the heat transfer interaction between the surface and a large reservoir of fluid whereas the latter denotes the interaction between the fluid and all the surfaces confining it [24]. The Rayleigh number is generally used to portray the laminar to turbulent transition in the natural convention flow problems [27]. The Rayleigh number will be further discussed in section 6.3.

Radiation

Heat transfer by radiation between the surfaces does not require a medium for its propagation. Its effect is visualized maximum when the surfaces are separated by perfect vacuum [27]. Here, energy is emitted by matter through the means of electromagnetic waves. Thermal radiation denotes the radiation emitted by the body at a temperature above absolute zero [28].

Radiation heat transfer is given by the Stefan- Boltzmann law, and is usually surface-to-surface radiation (shown by Equation 5.2.3). Thermal radiation taking place between two bodies depends on the difference between the fourth power of their absolute temperatures.

$$q = \sigma_{sb}(\varepsilon_1 T_1^4 - \varepsilon_2 T_2^4) \quad (5.2.3)$$

where A , ε , and T are surface area, emissivity and absolute temperature respectively of the body. σ is the Stefan-Boltzmann constant, which has a value equal to $5.67 \cdot 10^{-8} \text{ W m}^{-2} \text{ K}^{-4}$ [29].

5.2.2 Porous medium

Conduction and Flow

In most of the cases, as explained earlier, heat transfer might not occur only by one mechanism. Instead there would be a combination of mechanisms taking place. For a porous medium, heat transfer by conduction in the solid and fluid phases take place in parallel, hence there is no heat transfer from one phase to another [26]. This is valid only in cases when the assumption of fast equilibration of heat transfer between the phases is made [30].

Equation 5.2.4 and Equation 5.2.5 denote the equations for the solid phase and for the fluid phase respectively, where the radiation has been ignored.

$$(1 - \varphi)(\rho c)_s \frac{\partial T_s}{\partial t} = (1 - \varphi) \nabla \cdot (k_s \nabla T_s) + (1 - \varphi) q_s^m \quad (5.2.4)$$

$$\varphi(\rho c_p)_f \frac{\partial T_f}{\partial t} + (\rho c_p)_f \mathbf{v} \cdot \nabla T_f = \varphi \nabla \cdot (k_f \nabla T_f) + \varphi q_f^m \quad (5.2.5)$$

The subscripts s and f denote the solid and fluid phase respectively, c is the specific heat of the solid, c_p is the specific heat at constant pressure of the fluid, k is the thermal conductivity, ρ is the density and q is the heat production per unit volume [26]. Since heat transfer in both phases are parallel, Equation 5.2.4 and Equation 5.2.5 are combined to give Equation 5.2.6, where T_s and T_f equals T

$$(\rho c)_m \frac{\partial T}{\partial t} + (\rho c_p)_f \mathbf{v} \cdot \nabla T = \nabla \cdot (k_m \nabla T) + q_m^m \quad (5.2.6)$$

The second term on the left side of the Equation 5.2.6 denotes the transport of energy due to the fluid flow and the first term on the right side of the same equation is the net rate of heat conduction into a unit volume of fluid [26].

Overall heat capacity per unit volume, overall thermal conductivity and overall heat production per unit volume of the porous medium are defined by the equations Equation 5.2.7, Equation 5.2.8 and Equation 5.2.9 respectively [26]. Here φ is the porosity of the medium

$$(\rho c)_m = (1 - \varphi)(\rho c)_s + \varphi(\rho c_p)_f \quad (5.2.7)$$

$$k_m = (1 - \varphi)k_s + \varphi k_f \quad (5.2.8)$$

$$q_m^m = (1 - \varphi)q_s^m + \varphi q_f^m \quad (5.2.9)$$

Overall thermal conductivity depends majorly on the geometry of the porous medium. If heat transfer by conduction take place in series with the solid and fluid phases, overall thermal conductivity is given by the following equation [26]:

$$\frac{1}{k_m} = \frac{(1 - \varphi)}{k_s} + \frac{\varphi}{k_f} \quad (5.2.10)$$

Convection

For the case where there is porous media as well, convection is represented by Equation 5.2.2. Also the categories of free and forced convection exist depending on the driving forces.

Radiation

Radiation has the potential to penetrate even the porous material and serve as a volumetric heat source generation [29]. Radiation for the porous media is also represented by the Equation 5.2.3.

5.3 Mass transport

5.3.1 Fluid phase

Diffusion and Flow

Diffusion phenomenon is witnessed due to the concentration gradient established by the motion of the fluid species. To describe diffusion, Fick's law is appropriate to be used in the situation of pure fluids. The law states that the flux is directly proportional to the mole or mass concentration gradient. [24].

$$J_A^M = -cD_{AB,CF}\nabla x_A \quad (5.3.1)$$

c is the concentration, $D_{AB,CF}$ is the diffusion coefficient, J_A^M is the molar flux relative to the molar average velocity and x_A is the mole fraction of component A [24].

It is vital to consider that the molar flux, N_A , is a combination of the concentration gradient contribution (referred as diffusion) and the bulk motion contribution (referred as flow), shown in Equation 5.3.2 ,

$$N_A = -cD_{AB,CF}\nabla x_A + x_A(N_A + N_B) \quad (5.3.2)$$

$$c_A\mathbf{V} = x_A(N_A + N_B) \quad (5.3.3)$$

where $c_A\mathbf{V}$ is the molar average velocity and N is the molar flux relative to the stationary spatial coordinates. The first term on the right side of the Equation 5.3.2 is the molar flux which results from the concentration gradient, and the second term on the right of the same equation is the molar flux resulting as component A is carried in the bulk fluid flow [27].

Convection

Apart from mass transfer with diffusion and flow, convective mass transfer is another important category to be discussed. This mode of mass transfer describes that the mass transfer of fluid from the surface to adjacent fluid by the dynamic characteristics of the moving fluid. Convective mass transfer also involves transfer of species from its higher towards its lower concentration. Hence this category of mass transfer depends on both the transport properties and the dynamic characteristics of the moving fluid [27].

As in the case of convective heat transfer, there are two types involved. If the fluid motion occurs through the density differences, it is known as the free or natural convection. If the fluid motion occurs through the aid of an external device, then it is known as forced convection [27].

Analogous to the convective heat transfer rate equation (Equation 5.2.2), convective mass transfer is rewritten as,

$$N_A = k_c\Delta c_A \quad (5.3.4)$$

where N_A is the molar flux of species A relative to the fixed spatial coordinates, Δc_A is the concentration difference and k_c is the convective mass transfer coefficient [27].

5.3.2 Porous media

Diffusion and Flow

It is important to consider the interaction between diffusion and flow. For porous media, Knudsen diffusion is encountered in addition to the ordinary diffusion. Introduction of porous media factor to the Fick's law makes it suitable to be used in the cases to define ordinary diffusion in porous media. Equation 5.3.1 is modified by the addition of porous media factor β to be used for the porous media [24].

$$D_{AB,CF}^* = \beta D_{AB,CF} \quad (5.3.5)$$

$$\beta = \varphi S_g \tau \quad (5.3.6)$$

$$N_A = -c D_{AB,CF}^* \nabla x_A + x_A (N_A + N_B) \quad (5.3.7)$$

$D_{AB,CF}^*$ is the effective diffusion coefficient of the water vapour in a porous media, $D_{AB,CF}$ is the effective diffusion coefficient of the water vapour in pure fluids, φ is the porosity, S_g is the gas saturation (equal to 1.0 for all-gas conditions), and τ is the tortuosity. In Equation 5.3.7, the first and the second term on the right side represent the diffusion and flow term respectively. Tortuosity factor defines the ratio of length of the tortuous path to the straight line, which is predicted by different models. The most commonly used model is the Millington and Quirk model, which relates tortuosity to the one-third power of the porosity of the porous medium,

$$\tau = \varphi^{\frac{1}{3}} S_g^{\frac{7}{3}} \quad (5.3.8)$$

Knudsen diffusion refers to the diffusion when the mean free path of the fluid molecule is equal to the same order as the porous media pore diameter. Configurational diffusion is seen in cases where pore size decreases further and the size of the fluid molecule is equivalent to the pore diameter. The effect of porous media could be included by using Knudsen diffusion and configurational diffusion [24].

Convection

Convective mass transfer in porous media also depends on both the transport properties and the dynamic characteristics of the moving fluid. Similarly, there are two types of mass transfer involved - free and forced convection. The rate equation is represented by the Equation 5.2.2 [27].

5.4 Evaporation and Condensation

Evaporation and condensation have to be discussed when moisture transport results in phase transition. Evaporation of liquid requires energy, which is attained from cooling an object. The amount of energy required to transform the specified amount of liquid to gas is given by the enthalpy of vaporization [31].

Condensation is defined by the change of state from vapour to liquid when it comes in contact with a liquid or solid surface. In the process of condensation, energy is released from the vapour to liquid, and the amount of energy required to change the phase is the heat of condensation. Usually, condensation is said to occur if the gas is cooled or compressed, that is, in other words, it occurs when the vapour contacts the surface at a temperature below the saturation temperature of the vapour [27]. The definition of relative humidity is significant in understanding the phenomenon. Relative humidity (RH) is defined as the ratio of amount of water vapour in the air to the maximum amount of water vapour that could be present in the air at a particular temperature and atmospheric pressure. The atmospheric pressure is considered constant since the changes in pressure are generally very small and are neglected. Irrespective of the atmospheric pressure, there are noticeable changes in atmospheric temperature and the relation between the temperature and relative humidity (RH) could be checked in psychometric charts. Temperature and RH are inversely proportional. It is said that change of about 2% with RH is witnessed with every 1°F change in temperature. If there is a certain temperature and RH is 50%, further temperature changes up till the RH being 100% does not cause condensation. But further temperature decrease when the RH is already 100% would result in the concentration of water vapour in air to exceed above the saturation point and condenses as liquid droplets. This saturation point is referred to as the dew point[32]. The rate of condensation is increased with vapour temperature decrease and is also influenced by other parameters such as the surface area available for condensation and the wind speed in the environment. To summarize, effect of condensation is witnessed with the vapour temperature decrease, thus a resultant decrease in the vapour concentration and an increase in the liquid concentration.

6

Dimensionless numbers

Dimensionless numbers are used to give an overview of how a specific system will behave. In this study, they are used for parameter estimation involved in the transport processes. In addition to give an approximation about the vital transport processes in the model.

The relevant dimensionless numbers are presented here.

6.1 Reynolds number

The Reynolds number (Re) is the ratio of the inertial forces to the viscous forces in a fluid.

$$Re = \frac{\bar{u}L}{\nu} \quad (6.1.1)$$

\bar{u} and L are mean flow velocity and characteristic length of the flow geometry respectively. ν is the kinematic viscosity. Laminar flow is generally categorised by viscous forces and the turbulent flow is dominated by the inertial forces. If in case the Reynolds number is small, then the viscous forces would be larger than the inertial forces. Hence this dimensionless number is useful in characterizing whether the flow is laminar or turbulent. The critical Reynolds number, below which the flow is laminar, varies with geometry [28].

6.2 Nusselt number

The Nusselt number (Nu) is a dimensionless heat transfer coefficient, which is the product of the Reynolds number and the Prandtl number ($Nu = RePr$). The Prandtl number (Pr) is the ratio of momentum diffusivity to thermal diffusivity. To characterize the means of heat transfer, the Nusselt number is defined as the ratio of the heat flux including convection to the reference case of conductive heat flux [33].

$$Nu = \frac{q_{with\ convection}}{q_{reference\ case\ conduction}} \quad (6.2.1)$$

6.3 Rayleigh number

The Grashof number(Gr) is the ratio of buoyancy force to viscous forces. In the cases of free convection where the buoyancy forces dominate the flow, the Grashof number takes the place of the Reynolds number(Re) in the Nusselt number calculations ($Nu = RePr$). This combination of the Grashof number and the Prandtl number is termed as the Rayleigh number(Ra), shown in Equation 6.3.1 [24].

The Rayleigh number is used to characterise the means of heat transfer. In the case where it is lower than a critical value specific for a fluid, then the conductive heat transfer is said to be dominant. There is said to be convective dominant heat transfer taking place when Ra exceeds the critical value.

$$Ra = GrPr \quad (6.3.1)$$

$$Ra = \frac{\rho^2 c_p g \beta H^3 \Delta T}{\mu k} \quad (6.3.2)$$

β, μ, ρ and c_p are heat expansion coefficient, viscosity, density and specific heat capacity respectively. k denotes the thermal conductivity; H refers to the thickness of the layer; ΔT is the temperature difference existing in the layer [26]. The critical Rayleigh number for the pure fluids(air) is in the order 10^3 [34]. Whereas the critical Rayleigh number for the air within the porous media is in the order of magnitude 10^5 [35].

6.4 Stark/Stefan number

$$Sk = Sf = \frac{\varepsilon \sigma_{sb} T^3 L}{\lambda} \quad (6.4.1)$$

Where σ_{sb} is the Stefan- boltzmann constant, T is the temperature of the external environment, L is the characteristic length, λ is the thermal conductivity of the fluid and ε is the emissivity of the wall. This number define the ratio of the heat transfer by radiation to the heat transfer by conduction [36].

6.5 Hottel number

$$Hot = \frac{\alpha}{\varepsilon \sigma_{sb} T^3 L} \quad (6.5.1)$$

Where α is the convective heat transfer coefficient, σ_{sb} , T is the absolute temperature, ε is the emissivity. The Hottel number(Hot) denotes the ratio of heat flow by convection to the heat flow by radiation [36].

6.6 Peclet number

The Peclet number is significant to characterise the means of both mass and heat transfer.

It is the ratio of convection mass transfer to diffusion mass transfer. If the Peclet number (Pe) $\gg 1$, then convective term is dominant and as means of approximation, the diffusion mass transfer can be neglected.

$$Pe = \frac{UL}{D_m} \quad (6.6.1)$$

U and L are the flow velocity and length of the flow geometry and D_m is the mass diffusivity [37].

Similarly, the Peclet number for heat transfer is defined by the Equation 6.6.2. Here, k is the thermal conductivity. Pe is the ratio of convective heat transfer to conductive heat transfer. If $Pe \gg 1$, then the convective term is dominant and the conductive heat transfer could be ignored.

$$Pe = \frac{UL}{k} \quad (6.6.2)$$

7

Computational tool

The complete skin-product model is designed and analyzed with the help of the computational software COMSOL Multiphysics. COMSOL is a finite element analysis tool for modelling and simulating engineering problems. Being user-friendly, it is employed easily to analyze the physics involved in depth by providing the user access to the underlying equations [38].

8

Skin Model

Skin or any other body part is complicated to be involved in a study model since the body's internal mechanism is hard to be predicted. Irrespective of that, through a complete literature reading, it is understood that there are several ways to model the skin in a simplified manner having few assumptions taken into account. This section would discuss about the various existing skin models and the validity of the assumptions in reality.

Previous studies have used thermal manikins and human subjects for carrying out clothing comfort studies experimentally. Earlier, Gagge developed a two node (core and skin) model to explain the body's thermal regulation process. But it does not apply for the transient conditions since there is an assumption related to isothermal behaviour of the human body, clothing and the environment. Li and Holcombe combines the Gagge model with the sorption kinetics of the clothing [39]. They evaluate the problem using the mathematics as a tool and consider the human body as two concentric shells, that is, the inner core and the outer skin. In the study by Wang et al., a numerical manikin is used where a heat flux pertaining to the metabolic activity level and an emissivity at the body surface are specified [2]. The Berkley Comfort model considers the body divided into 15 segments where each segment is divided into four nodes (skin, core, vein blood and artery blood) and uses the Penne's bio heat equation to involve the body's thermoregulation system. The model takes into consideration the metabolic heat source, blood perfusion rate, arterial temperature, density and specific heat of the blood [40]. The Berkley Comfort model can be a potential basis for the study, but in-depth knowledge of the human circulatory system is beyond the project scope as it is sufficient to find a relevant skin model which allows for necessary product properties to be simulated. An interesting approach is noticed in the analysis made by Huang et al. and Zhang et al. where the temperature and RH near the skin surface and external environmental conditions are specified [1, 41]. In addition to such conditions, effective wind speed has been also an input in another study [4]. Two groups, Celcar et al. and Meinander focused on the measurement of heat and moisture transmission through clothing using a sweating cylinder. Here, different sweating levels are considered on the skin surfaces along with the specified environmental conditions [42, 43].

The model in this project investigates two approaches of representing the skin where in both the cases, it is described as a surface or boundary. The first approach is to consider constant skin temperature and constant RH near the skin, motivated from

the article by Huang et al. [1]. The information for prediction of RH near skin is not enough and hence a sub model is made to predict the RH near the skin. In the sub model, model inputs of skin diffusive flux and skin temperature are fed as constant parameters. The approach in the sub model is seen to be similar to the articles [42, 43], but with further modifications such as the sweating manikin being replaced by a skin surface and the experimental aid for analysis being replaced with the computational power.

9

Complete Model

9.1 Model Geometry

The complete model in COMSOL is visualized consisting of two different domains. It explains the transport processes taking place between the skin and the product and within the product. The product is exposed to the outer environment. The skin and the product are separated by an air layer.

From Chapter 8, it is concluded that the skin will be modelled as a boundary. The skin is shown highlighted in the Figure 9.1.1 by a red colour line denoted as A. A-B in the model represents the air layer, which is highlighted as a grid shaded region. From Chapter 3, it has been analysed to consider only the product's absorbent core as a single layer to denote the product in the model. The absorbent core of the product is represented by a porous domain (B-C), shown as a dot shaded region. B denotes the inner boundary of the porous domain, marked by a black line. The back sheet (commonly called the film) of the product is too thin to be modelled as a separate domain, as meshing very small domains accurately would result in very large computation time. Hence, the product's back sheet (film) is assumed to be a boundary on the outer surface of the porous domain. The film is marked by blue colour in the figure. The surrounding environment which is present after the outer boundary of the porous domain is modelled as a virtual domain.

To sum up, the entire model is seen as two domains :

- Domain A-B : 5 mm air layer between the skin boundary and the inner boundary of the porous domain.
- Domain B-C : 7 mm porous domain with its outer boundary defined as the film.

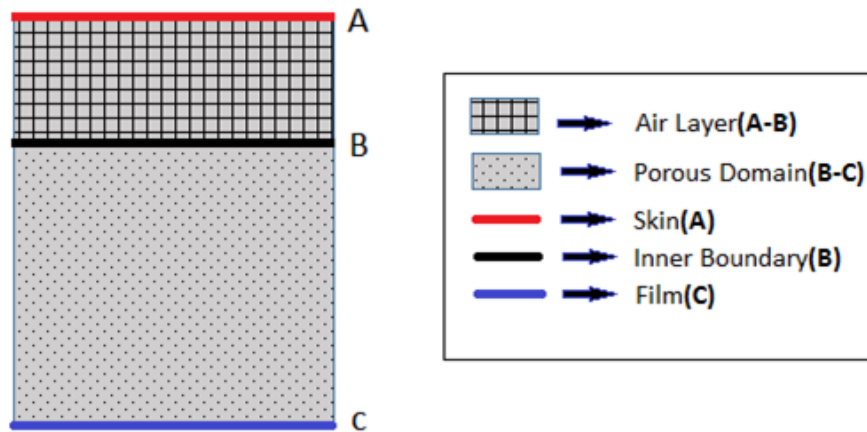


Figure 9.1.1: Model Geometry

9.2 Model Assumptions

There are assumptions made in the model in order to avoid complexity of understanding few processes. The assumptions are as follows:

- The product is drawn as a 2D model geometry. Since the scope is to analyse the transport processes, either 1D or 2D model would suffice the purpose.
- The study in the project is carried out in the steady state.
- The body wearing the diaper is assumed to be naked, so there is no clothing layer adjacent to the diaper back sheet, which otherwise would be an additional resistance to the transport processes.
- The product is said to have a homogeneous fiber structure, resulting the material properties to remain constant throughout the medium.
- A design of simplified model with standing baby wearing the product in the room, is aimed. Hence there is no consideration of wind speed.
- Dry state product is said to be used in the analysis.
- The product is assumed to be a rigid structure. Hence swelling of product structure due to moisture transmission is neglected, thereby permeability and porosity of the porous medium remains constant.
- It would be difficult to analyze all of the transport processes within the model. For modelling simplifications, wicking has been ignored since the onset of condensation is of major interest.

9.3 Model Data

Data required for the model is fed in through literature searches. Material data for the air is found default in COMSOL. Through an initial literature search, material data for the porous domain are manually entered. The porous domain is approximated to consist of cellulose fibres and the film has been assumed to be composed of polyethylene. The material properties are shown in the Table 9.3.1.

Material	$\rho(\text{kg/m}^3)$	$k(\text{W/m K})$	$C_p(\text{J/kg K})$	$\varepsilon(\text{Emissivity})$
Porous domain	900 ^[44]	0.06 ^[45]	1700 ^[46]	0.95 ^[47]
Film	920 ^[45]	0.33 ^[48]	1900 ^[45]	0.1 ^[49]

Table 9.3.1: Material Data

Here, ρ , k , C_p , ε represents the density, thermal conductivity, specific heat capacity and emissivity respectively. For the pre-study, the permeability and porosity of the porous domain are assumed 10^{-11} m^2 and 0.8 respectively [25]. The diffusion coefficient of the water vapour in the film is calculated using the Mocon number (Appendix A1). The Mocon number quantifies the breathability of the film by measuring the water vapour transmission rate (WVTR). It is not a dimensionless number and $\text{g/m}^2 24h$ is its unit.

9.4 Meshing and Solvers

Meshing is the second step to be followed after drawing the geometry. A finer mesh is aimed with 33572 triangular elements using the meshing technique 'free triangular'. Average mesh quality is check with the mesh statistics and is estimated as 0.993.

Solver parameters are set just before the simulation step. PARADISO is chosen as the stationary solver in the model and the relative tolerance is set to 0.001.

9.5 Physics and Boundary Conditions

9.5.1 Momentum Transport

In this case, there are two possible driving forces for flow - pressure gradient and gravity. Since the system is exposed to the surrounding atmospheric pressure, the pressure differences are considered to be negligible. Using Equation 5.1.2 the flow due to gravity is found to be as low as 10^{-6} m/s . Using the Rayleigh number, the

transport due to flow can be shown to be negligible in comparison to transport due to conduction. Accordingly the flow component is neglected in the model.

9.5.2 Heat Transport

Heat transfer by conduction, flow, convection and radiation is modelled through an interface 'Heat transfer in Porous media' in COMSOL [50]. Convection is less dominant in the model and is ignored. The interface gives the possibility to define 'heat transfer in fluid' in domain 1 and 'heat transfer in porous medium' in domain 2. Skin is assumed as a boundary with constant temperature. The ambient environment outside the porous domain is assumed to remain constant at a lower temperature when compared to the skin temperature. The initial temperature in both the domains is set to be the ambient temperature. Heat transfer in general takes place due to the existence of a temperature gradient, wherein the transfer takes place in the direction from higher temperature to the lower temperature. This makes it evident that at the initial stage, there is transfer of heat from the skin towards the porous domain. The equations in the fluid domain and the porous domain are slightly different, shown by Equation 9.5.1 and Equation 9.5.2 respectively. The first term on the left side is eliminated due to the flow being neglected. Q on the right side of equations refer to the heat source/sink terms. Q_p and Q_{vd} refer to the work due to pressure changes and the viscous dissipation term respectively but both the terms are eliminated due to the negligible flow. Since the equations are solved in steady state assumption, the temperature does not change with time, hence the time derivative term is eliminated in both of the equations. The effective thermal conductivity of the porous media depends on the porosity of the porous medium, which is seen in the Equation 9.5.3. k_{eff} refers to the effective thermal conductivity of the porous medium and the porous medium. ϵ denotes the porosity of the porous medium.

$$\rho c_p \mathbf{u} \cdot \nabla T - \nabla \cdot k \nabla T = Q + Q_p + Q_{vd} \quad (9.5.1)$$

$$\rho c_p \mathbf{u} \cdot \nabla T - \nabla \cdot k_{eff} \nabla T = Q + Q_p + Q_{vd} \quad (9.5.2)$$

$$\frac{1}{k_{eff}} = \frac{1 - \epsilon}{k_p} + \frac{(\epsilon)}{k} \quad (9.5.3)$$

Here, k , k_p denotes the thermal conductivity of the fluid and the solid porous material respectively. \mathbf{u} denotes the flow velocity. ∇T is the temperature gradient. Since there is no flux involved across the vertical boundaries of the domains, symmetry is set as a condition at those boundaries, which is explained by the below equation [50]. All the module boundary conditions are seen in Appendix A2.

$$-\mathbf{n} \cdot \mathbf{q} = 0 \quad (9.5.4)$$

Heat transfer through the film is accounted for imposing a heat flux boundary condition at the outer surface of the product. The boundary is defined as a thin porous layer with certain thickness d_s and conductive property k_s (see Equation 9.5.5 and Equation 9.5.6).

$$q = -\frac{k_s}{d_s}(T_{amb} - T) \quad (9.5.5)$$

$$\frac{1}{k_s} = \frac{(1 - \epsilon_f)}{k_f} + \frac{\epsilon_f}{k_{air}} \quad (9.5.6)$$

where T_{amb} refers to the ambient temperature, ϵ_f and k_f denotes the porosity and conductivity of the film; k_{air} refers to the thermal conductivity of air. The thickness of the film for the initial study is assumed to be $18 \mu\text{m}$ [25]. The porosity of the film is calculated with the Mocon number of the film and is found as 0.00074 for a highly breathable film (Appendix A2). The rest of the film parameters are given in Table 9.1.

Radiation

Surface-to-surface radiation is included in the heat transfer equation through the heat source or sink term Q , seen in Equation 9.5.1 and Equation 9.5.2. Diffuse surface boundary conditions are incorporated in the model in order to include effects of surface-to-surface radiation. The diffuse surface adds radiative heat source contribution on the boundary side where radiation is defined, shown in Equation 9.5.7. Radiative heat source is incorporated on both sides of the diffuse boundary if the radiation is defined on both sides [50].

$$q = G - \epsilon\sigma_b(T) \quad (9.5.7)$$

where G is the incident radiation and the second term on the left side of the Equation 9.5.7 refers to the radiation leaving the surface.

Three diffuse surfaces have to be added to the model, which includes the skin, the inner boundary of the porous domain and the outer boundary of the porous domain. With the calculation of the Stark number, adding radiation source on the film gives no effect. Hence it is concluded to define only two diffuse surfaces to account for radiation. The porous domain is opaque, which leads to the specification of opacity controlled direction to the diffuse surface at the inner boundary of the porous domain. The emissivity values of the materials are given in Table 9.3.1. Among the diffuse surfaces, skin is the main source of radiation and it is necessary to analyse the heat emitted from human body for this project. The emissivity is found to be 0.99, stating it as a black body [49]. Symmetry boundary condition applies for radiation as well, since there is no radiative flux across the ends of the domains.

The important boundary conditions in the heat transfer section is summed up in Figure 9.5.1

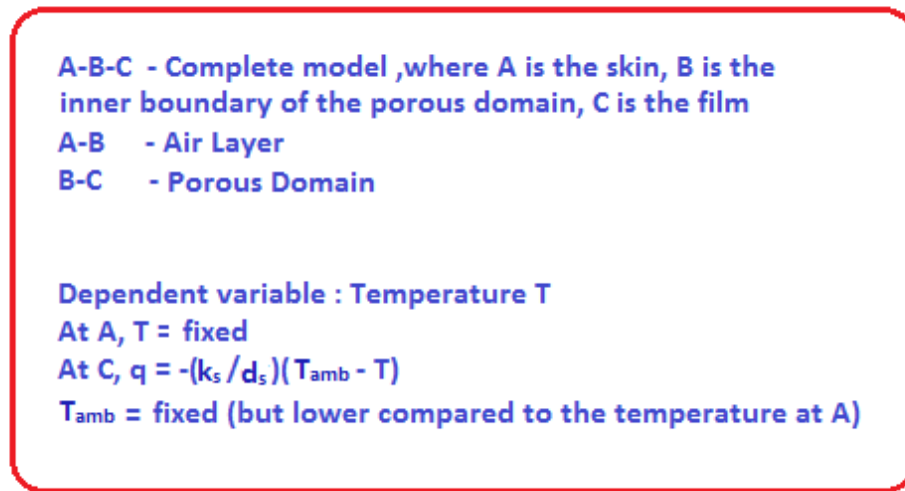


Figure 9.5.1: Boundary conditions

9.5.3 Mass Transport

Mass transfer of water vapor in air is investigated in the model. COMSOL's interface 'Transport of diluted species' is a potential interface which could be used since it is used to calculate the concentration gradient of the dilute solute in a solvent. The mechanism for the mass transport is diffusion, and when coupled to the flow field, convection could also be included as an effect in the mass transport processes [50]. But in this study, convection is neglected. The interface gives the flexibility to model the mass transport processes in the fluid domain and the porous domain, just like the heat transfer physics.

The skin is defined to emit certain concentration of water vapor in the model. The concentration is calculated from the RH near skin, which is fixed through simulations to attain a certain diffusive flux from the skin. Diffusive flux from the skin is called the EW in this study. EW accounts for only TEWL or both TEWL and evaporated sweat. There are some validated TEWL range studied from literature and it is taken into account for the model simulations to attain a starting point with the RH near the skin. The ambient environment is assumed to have a lower vapour concentration when compared to the vapour concentration near the skin. The concentration of water vapor at the skin and at the ambient are calculated from the RH near skin and the ambient RH respectively (Appendix A1). The initial concentration in both the domains is set to the ambient concentration. Mass transfer takes place due to the concentration driving forces in the model, where the transfer processes are governed by Equation(9.5.8) and Equation(9.5.9) in the fluid domain and the porous domain respectively.

$$\nabla \cdot (-D_i \nabla c_i) = R_i \quad (9.5.8a)$$

$$\mathbf{N}_i = -D_i \nabla c_i \quad (9.5.8b)$$

$$\nabla \cdot \mathbf{\Gamma}_i = R_i + S_i \quad (9.5.9a)$$

$$\mathbf{N}_i = \mathbf{\Gamma}_i = -D_{e,j} \nabla c_i \quad (9.5.9b)$$

In the (9.5.8), R_i denotes the mass source/sink term; S_i refers to the source term added for the species involved in the transport; diffusion coefficient of water vapor in air is entered as a variable dependent on the model temperature, which is shown in Appendix A1. The diffusion coefficient of water vapour through the porous medium ($D_{e,j}$) seen in the (9.5.8) is defined below.

$$D_{e,j} = \frac{\epsilon_p}{\tau_{f,j}} D_{f,j} \quad (9.5.10)$$

$D_{f,j}$ is fluid diffusion coefficient. The tortuosity is given by the Millington-Quirk Model, same as explained before in Equation 5.3.8. The mass transfer through the film is modelled by imposing a boundary condition of flux. The film is modelled as a thin diffusion barrier. The structure could be assumed similar to the porous medium but with a lower porosity than the porous medium. The equation depicting the diffusion through film is shown below, where the diffusion coefficient of water vapour in the film is calculated with respect to the Mocon number (Appendix A1).

$$N = -\frac{D_b}{d_s} (C_{amb} - c) \quad (9.5.11)$$

d_s and D_b denotes the thickness of the film and the diffusion coefficient of water vapour through the film respectively. C_{amb} is the ambient concentration; c is the concentration(mass transport dependent variable).

Symmetry at the vertical boundaries of the domains is taken into consideration in this model as well, since there is no diffusive flux across the vertical boundaries of both the domains. The symmetry node explains the equation, as seen below. The boundary condition is denoted in the Appendix A2.

$$-\mathbf{n} \cdot \mathbf{N}_i = 0 \quad (9.5.12)$$

The important boundary conditions in the mass transfer section is summed up in Figure 9.5.2

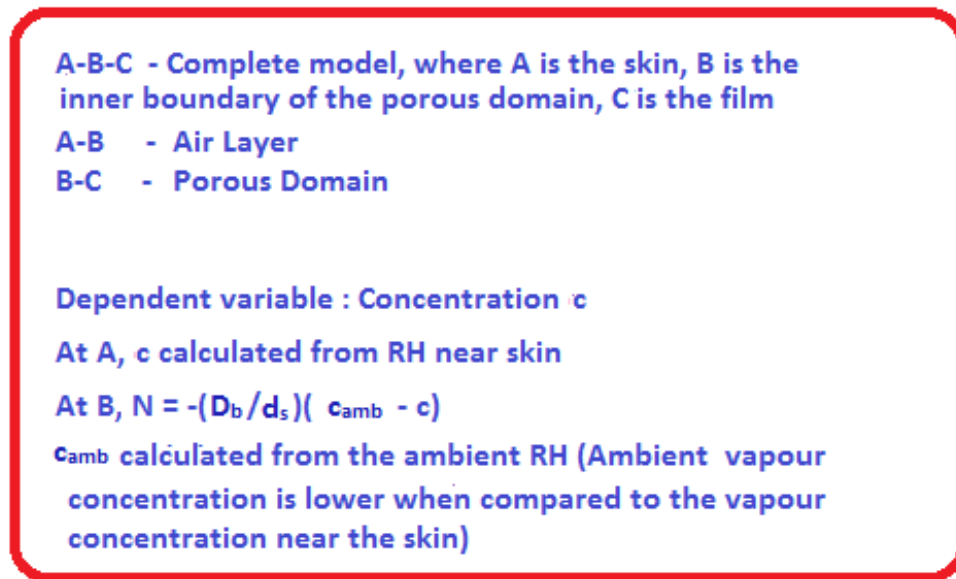


Figure 9.5.2: Boundary conditions

9.5.4 Condensation

Adsorption is a surface based process referring to the adhesion of molecules onto a surface. It is a transient process and can catalyse condensation, which is a continuing process. Condensation is said to modify the steady state and the heat flows involved [4]. Since the model is studied in its steady state, condensation phenomenon alone is analysed.

Condensation, as discussed earlier, is bound to happen when the vapour concentration is greater than the saturation vapour concentration. The excess vapour is condensed as liquid on the surface, for example, on the solid surface inside the porous medium. Due to condensation, heat loss and moisture loss is seen in the vapour phase. One way to model the phenomenon of condensation could be to add the heat sink and mass sink terms to the heat transfer and mass transfer equations respectively. This approach could be to some extent similar to the article by Lotens et. al. [4].

In COMSOL, condensation is governed by adding a reaction term to the porous domain in the interface 'Transport of diluted species'. In Equation(9.5.8), R_i refers to the reaction term, which is explained as follows:

$$R_i = -k(c - c_{sat})(c > c_{sat}) \quad (9.5.13)$$

$$c_{sat} = \frac{P_{sat}}{RT} \quad (9.5.14)$$

where c , c_{sat} , P_{sat} , R and k denotes the vapour concentration, saturation concentration, saturation pressure, universal gas constant and condensation rate respectively. Saturation pressure and saturation concentration are calculated through COMSOL. Condensation rate is assumed 100 s^{-1} for the pre-study. The condition ($c > c_{sat}$) is used to generate the whole reaction term active only when c is greater than c_{sat} . This is the case when condensation is bound to happen.

Similarly, a heat source term is added only to the porous domain in the COMSOL interface 'Heat transfer in Porous media'. In Equation 9.5.2, Q refers to the heat source term and is defined as shown:

$$Q = -H_{cond} * R_i \quad (9.5.15)$$

where H_{cond} refers to the heat of condensation taken as 43740 J/mol for water [4]; R_i refers to the reaction term described above. The heat source term is also seen to be activated only during the case of condensation, that is, when c is greater than c_{sat} .

10

Post Analysis

10.1 Skin as a boundary

It is explained previously that that boundary condition for the skin is to specify certain temperature and certain RH at the surface. Through literature studies, temperature at the skin surface is found to range from 28 to 35°C. The RH near the skin has been difficult to be predicted, and hence as mentioned before it is attempted to be found through an approach with constant skin diffusive flux and skin temperature as inputs. Diffusive flux from the skin is called EW in the study. EW accounts for either the TEWL or both TEWL and the evaporated sweat.

Some validations taken from the literature are used as a base for the model study. Having a certain RH near the skin is necessary in order to attain the appropriate range of TEWL from skin. From literature reading, TEWL from the skin is measured when it is not occluded by any clothing under specific ambient atmosphere conditions. The ambient atmosphere in the room is maintained at around 30-50% RH and at a temperature range of around 20-22°C [51]. Subjected to these conditions, the skin is measured to have a surface temperature of about 30-32°C. TEWL measurements are said to be appropriate when the above atmospheric conditions are maintained and is measured experimentally through instruments. TEWL is said to be in the range of 10-20g/m²h [51]. The values could also account for some evaporated sweat if the TEWL value is seen higher.

Even if the above ambient conditions are maintained, by reality it can be assumed for the body to sweat when the skin is occluded with the porous medium. As a result of which, EW is assumed to account for some evaporated sweat in addition to the TEWL. Hence the value of 10-20g/m²h is assumed to raise and cannot be estimated exactly. Nevertheless, to start with, it is decided to make the first study with EW of 10-20g/m²h to could go up to the range of 10-40g/m²h if the skin is occluded with materials.

The film occluding the skin should be to an extent breathable. The range of Mocon number for the breathable film investigation is decided to be 3000 g/m²24h and higher, and in the study it is decided to start with the Mocon number of 5000 g/m²24h [52]. The study does not concern with exact values since it is aimed to understand the underlying concepts. When maintaining the above conditions

with the assumptions, RH near skin is predicted to be in the range 50-70% (see Table 10.1.1). Nevertheless, the ambient temperature and the skin temperature could also affect the RH near the skin. It is concluded that the RH near the skin is dependent on the ambient RH, skin temperature, ambient temperature and the EW. But in order to analyse and compare the effect of heat and mass transfer in the complete model, it is assumed to proceed with a single random case. The case is kept as skin temperature of 32°C, RH near skin as 50%, ambient temperature of 22°C, and ambient RH of 40%. The parameters could be varied later in the analysis.

Trials	Ambient Temperature(°C)	Ambient RH (%)	Skin Temperature(°C)	RH near skin (%)	EW (g/m²h)
1	22	40	32	41	14
2	22	40	32	52	22.6
3	22	40	32	55	25
4	22	40	32	60	29
5	22	40	32	65	33
6	22	40	32	70	37

Table 10.1.1: EW corresponding to the RH near skin

10.2 Heat Transport

To investigate the effect of heat transfer, the 2D surface temperature profile, as in Figure 10.2.1, and the 2D cut line temperature profile, as in Figure 10.2.2, are visualised in the model. Cut line is made across the middle of the 2D model. These figures clearly show the gradual temperature decrease throughout the model, that is caused due to the higher skin surface temperature and the lower ambient temperature.

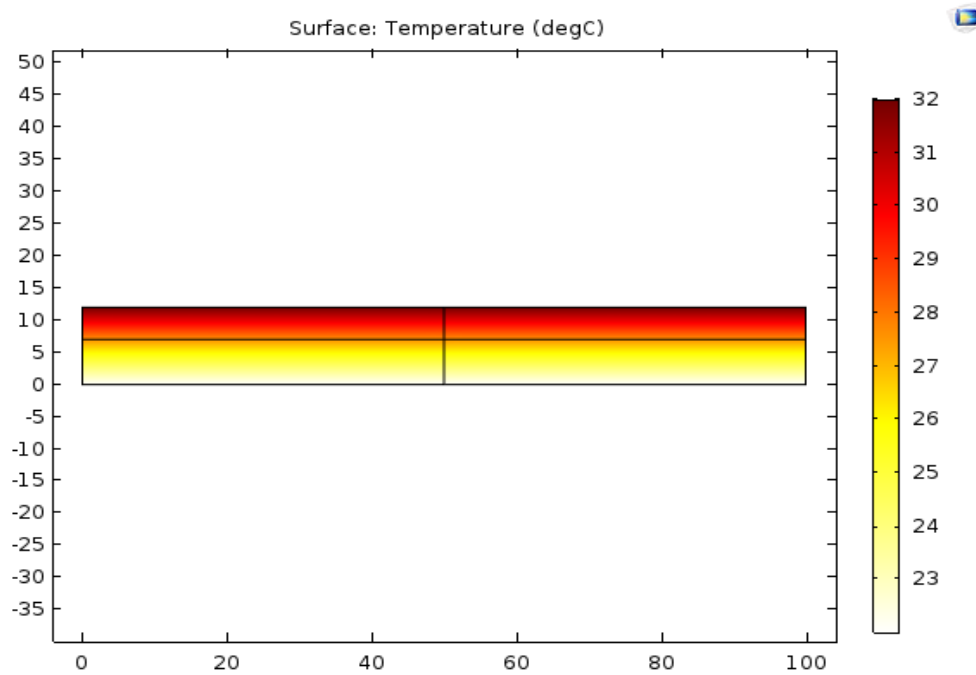


Figure 10.2.1: 2D Surface Temperature Profile

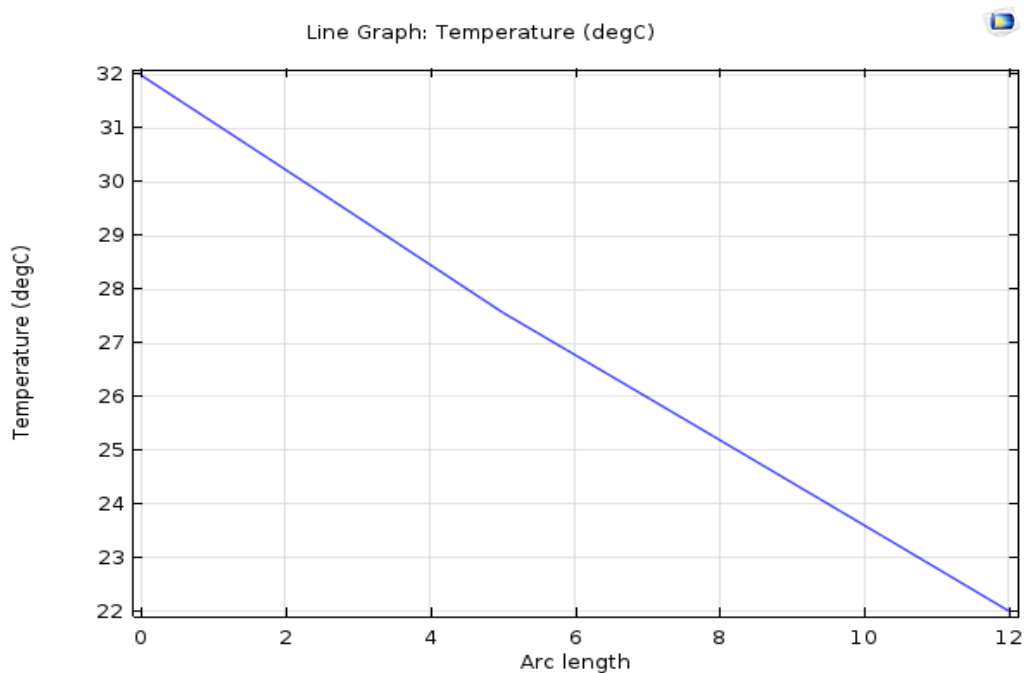


Figure 10.2.2: 2D Cut line Temperature Profile

Observing the Figure 10.2.2, the temperature is seen to decrease from 32°C at the skin surface to 27.3°C at the inner boundary of the porous domain, then further decreases to 22°C at the outer boundary of the porous domain. The linear temperature drop between the skin surface and inner boundary of the porous domain

has a different slope compared to the temperature drop between the inner and the outer boundary of the porous domain. This is explained due to the restriction for energy transfer within the porous material relative to the pure fluids. Since there is no convective flux present within the system, the flux balance in the model is solely due to the conductive flux, which is reported as 23.7 W/m^2 (Figure B.1.1). There is a negligible temperature drop across the film. This is explained by the thickness and the transport coefficient. Very low thickness and high conductivity at the outer boundary is the reason to such behaviour.

	Skin	Inner boundary of the porous domain	Outer boundary of the porous domain
Surface Temperature($^{\circ}\text{C}$)	32	27.3	22

Table 10.2.1: Heat Transport

10.3 Mass Transport

To investigate the effect of mass transfer, the 2D surface concentration profile, as in Figure 10.3.1, and the 2D cut line concentration profile, as in Figure 10.5.6, are visualised in the model. Cut line is made across the middle of the 2D model. These figures show the gradual concentration decrease throughout the model similar to the temperature curves, due to the higher skin surface vapour concentration and the lower ambient vapour concentration. Similar temperature and vapour concentration behaviours are seen across the model. The diffusion coefficient is set as a temperature dependent variable.

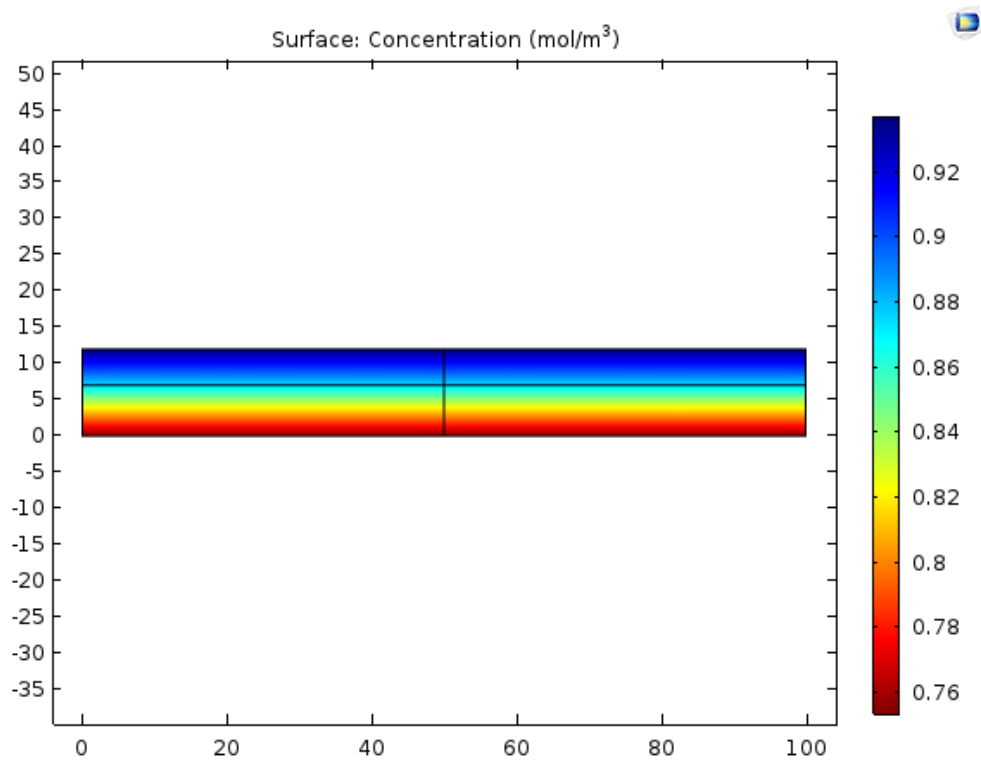


Figure 10.3.1: 2D Surface Concentration Profile

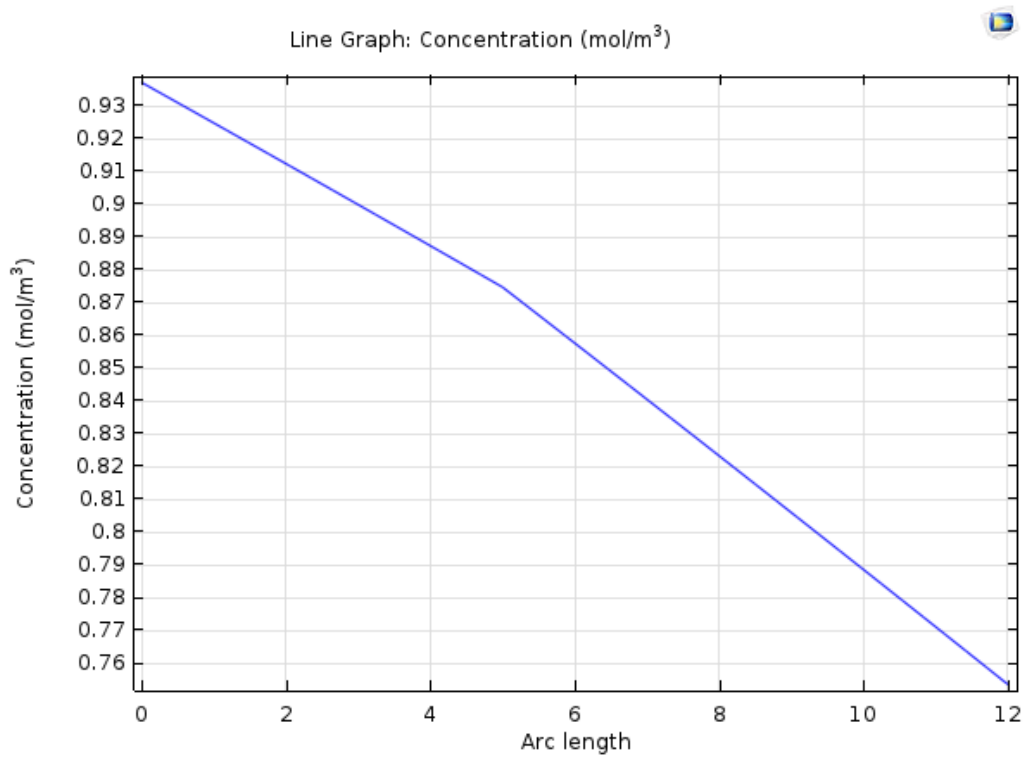


Figure 10.3.2: 2D Cut line Concentration Profile

Diffusive flux of around $20.9 \text{ g/m}^2\text{h}$ is witnessed throughout the model with the vapour concentration is seen to decrease from 0.94 mol/m^3 at the skin surface to 0.87 mol/m^3 at the inner boundary of the porous domain, then it further decreases to 0.75 mol/m^3 at the outer boundary of the porous domain (Figure 10.5.6, Figure B.1.2). Due to the diffusive ability being lower within the porous domain when compared to the pure fluid layer, the concentration drop is seen higher within the porous domain. Across the film, there is a concentration drop of 0.32 mol/m^3 . The higher concentration drop is explained by the film being the major diffusive barrier in the model.

	Skin	Inner boundary of the porous domain	Outer boundary of the porous domain	Ambient
Surface Vapor Concentration(mol/m³)	0.94	0.87	0.75	0.43

Table 10.3.1: Mass Transport

10.4 Effect of Radiation

To check for the effect of radiation in the heat transport, two cut line 1D plots are created highlighting the model with and without radiation (see Figure 10.4.1). The model with radiation is activated by introducing the diffuse surfaces and the condition surface-to-surface radiation, as explained in the section 9.5.2.

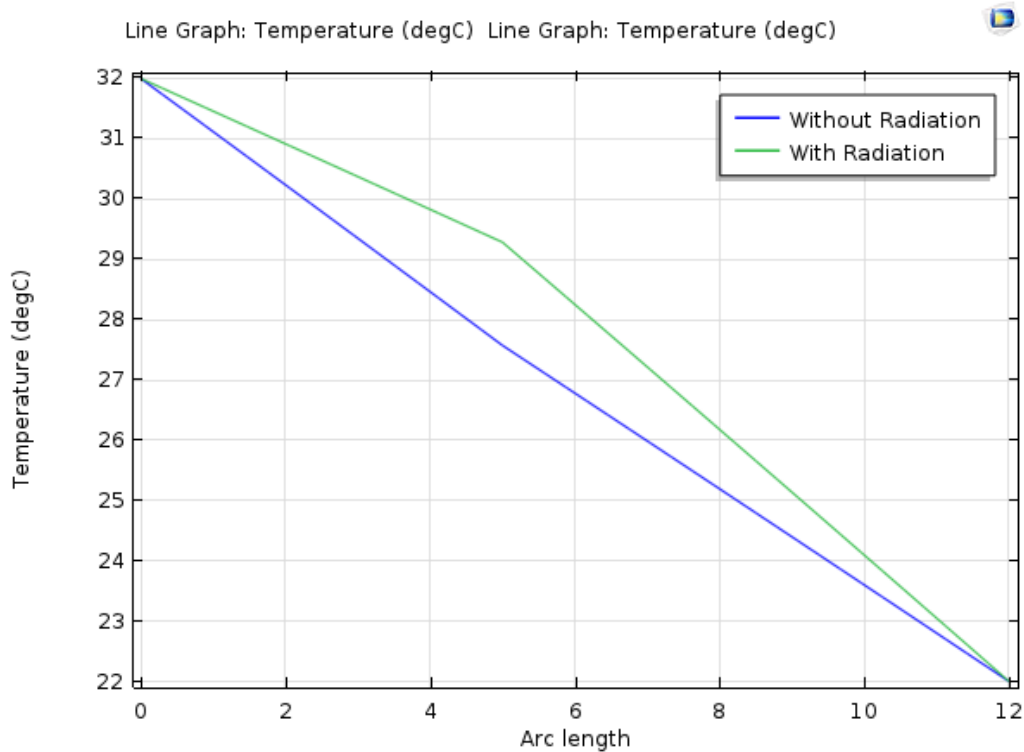


Figure 10.4.1: Effect of Radiation

Surface radiosity pertains to the radiation leaving the surface, which is checked for the activated diffuse surface in the radiation model. From Appendix B, it is seen that the skin surface emits at about $492\text{W}/\text{m}^2$ towards the direction of porous domain. Similarly it is noticed that the inner boundary of the porous domain emits radiation of about $475\text{W}/\text{m}^2$ towards the skin. The difference between them is the net radiation flux from the skin since the radiation emitted from the skin is higher compared to the radiation emitted from the inner boundary of the porous domain. The flux balance is investigated in the radiation model. The normal radiative flux and the conductive flux from the skin are estimated to $16\text{W}/\text{m}^2$ and $15\text{W}/\text{m}^2$ respectively. Out of the total flux from the skin, radiative flux accounts for about 52%. Such high contribution from the effect of radiation influences the energy transfer, and also modifies the surface temperature within the radiation model. Looking at the Table 10.4.2, a higher temperature drop within the porous domain is witnessed accounting for the higher rate of heat transfer, thus explaining the higher surface temperature at the inner boundary of the porous domain. It is understood that the inner boundary of the porous domain is cooler if radiation is not included in the model. As the temperature rise of about 2°C is an accountable temperature rise when compared to the overall temperature difference in the model, it demands the necessity to include the effect of radiation in the model for the following study.

	Without Radiation	With Radiation
Skin Temperature($^{\circ}\text{C}$)	32	32
Temperature of the inner boundary of the porous domain($^{\circ}\text{C}$)	27.3	29.2
Temperature of the outer boundary of the porous domain($^{\circ}\text{C}$)	22	22

Table 10.4.1: Effect of Radiation, as depicted in Figure 10.4.1

	Without Radiation	With Radiation
Temperature of the inner boundary of the porous domain($^{\circ}\text{C}$)	27.3	29.2
Temperature of the outer boundary of the porous domain($^{\circ}\text{C}$)	22	22
Temperature Drop across Porous domain($^{\circ}\text{C}$)	5.3	7.2

Table 10.4.2: Effect of Radiation

10.5 Effect of Condensation

To check for the effect of condensation in the transport processes, two cut line 1D plots are created highlighting the model with and without condensation. Here both the models include radiation effects since it has been discovered that radiation has a significant effect and is included in the further analysis. Condensation, as discussed before, is activated in the model by introducing a heat source term and a reaction term. The check for condensation happening in a model is visualized by looking closely at the vapour saturation concentration (c_{sat}) and vapour concentration (c) cut line 1D plots. In the cases where the vapour concentration is higher than the vapour saturation concentration, condensation occurs.

10.5.1 Varying ambient and skin parameters

With the base case where the skin temperature, RH near the skin, the ambient temperature and the ambient RH are 32°C , 50%, 22°C and 40% respectively, condensation is not witnessed since the vapour concentration has not exceeded the dew point (c curve is below the c_{sat} curve) throughout the model (Figure 10.5.1). This ultimately explains the zero heat source term and the zero reaction term. There is no change in temperature and concentration curves irrespective of the condensation effect activated (Figure 10.5.2 and Figure 10.5.3). Hence the total heat flux (conductive, radiative) and total mass flux (diffusive) is the same. If condensation happens, the percentage of moisture condensed can be found from the model through the

diffusive fluxes (see Equation 10.5.1)

$$\text{Moisture condensed}(\%) = \frac{\text{Diffusive flux at the skin} - \text{Diffusive flux at the film}}{\text{Diffusive flux at the skin}} \quad (10.5.1)$$

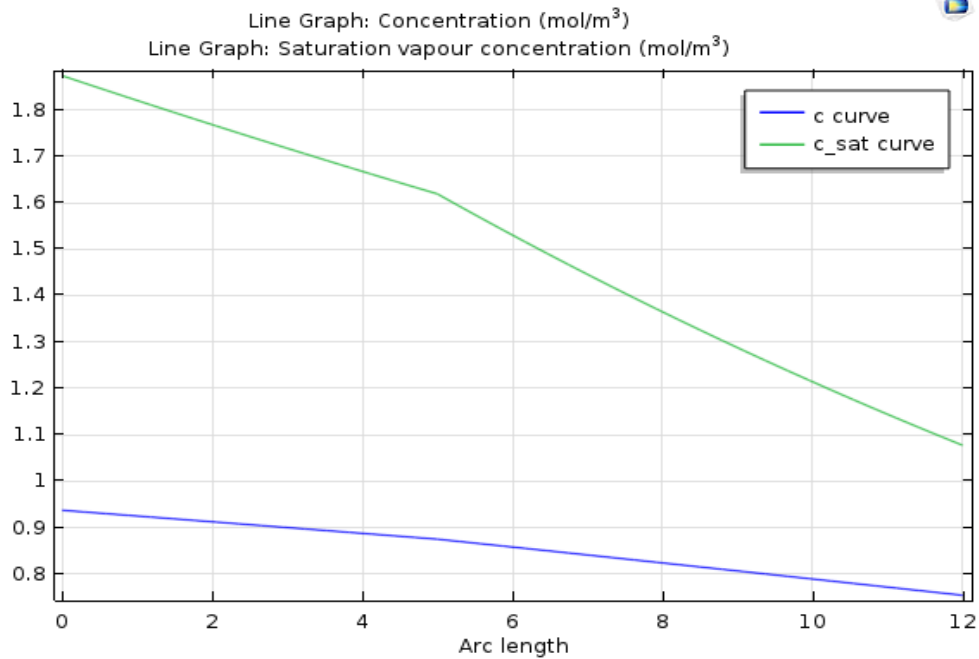


Figure 10.5.1: Base case - c and c_{sat} curve comparison

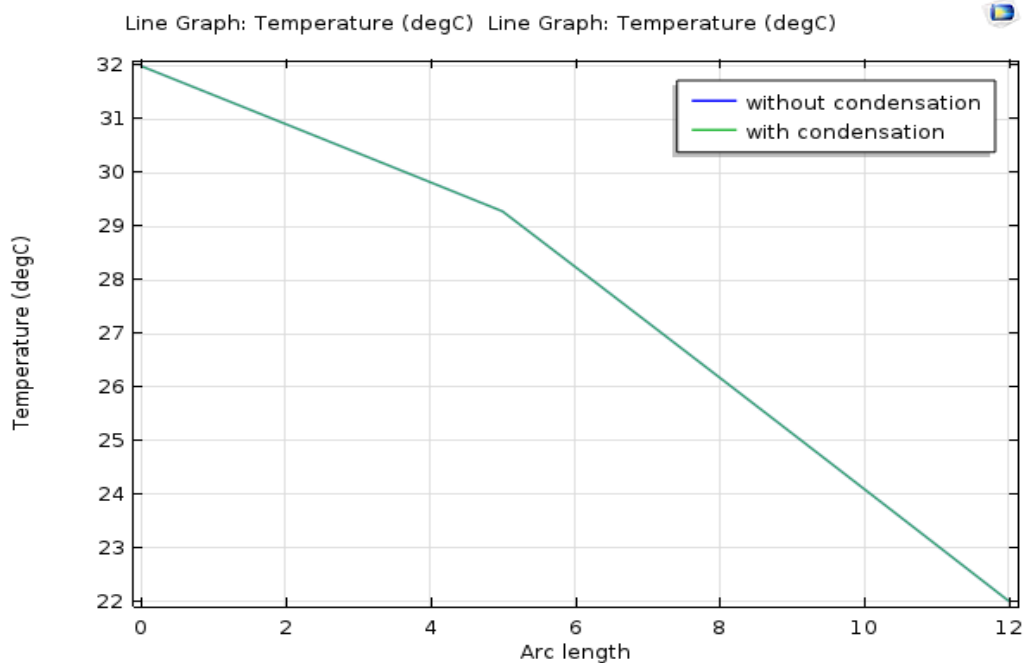


Figure 10.5.2: Base case - Temperature curve

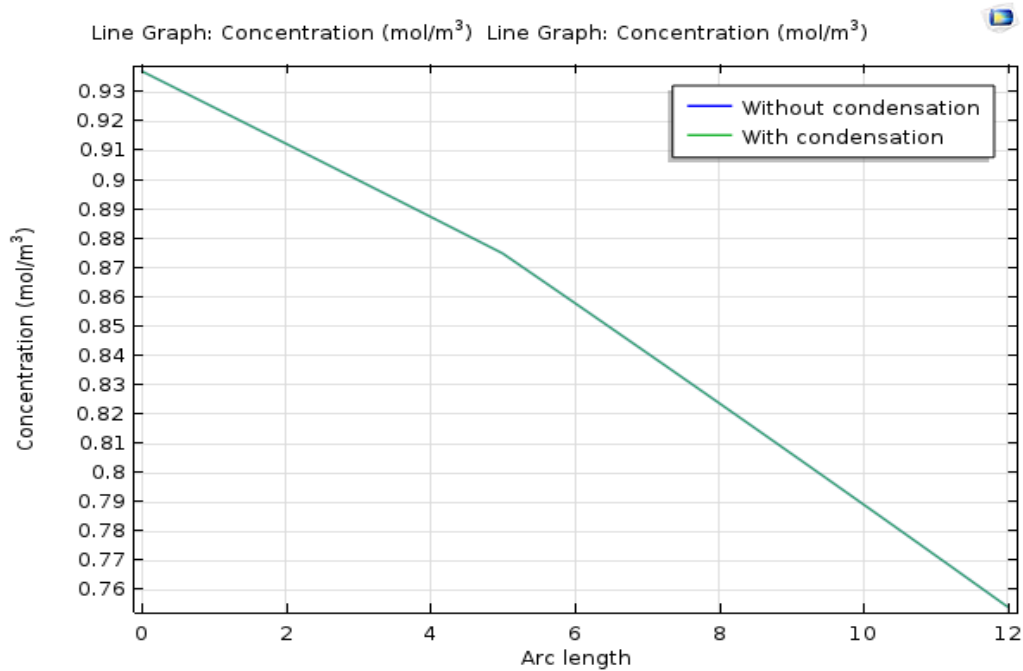


Figure 10.5.3: Base case - Concentration curve

From the literature, it is understood that a lower ambient temperature and a higher ambient humidity is expected to show condensation effects. To investigate the above statement, the ambient parameters are separately varied and the conclusions are made. The other model inputs such as the skin parameters are also varied to check for the effect of condensation. The following section analyses the four model inputs in detail - ambient temperature, ambient RH, skin temperature, RH near skin. In each study, one of the model input is varied and the other three are kept constant.

In study 1, the ambient temperature is varied in the range 10°C to 26°C, the other parameters are kept constant (ambient RH = 40%, skin temperature = 32°C, RH near skin = 50%). When decreasing the temperature from 26°C to 18°C, no effect of condensation is seen. On further decreasing the temperature, the percentage of condensed moisture increases with the temperature decrease (Figure 10.5.4). The underlying reason is the temperature being lowered to a point where the moisture gets condensed.

S.No	Skin Temperature(°C)	RH near skin (%)	Ambient Temperature(°C)	Ambient RH (%)	EW (g/m ² h)	Moisture condensed (%)	Location of condensation start (mm)
1	32	50	26	40	16.7	0	-
2	32	50	22	40	20.9	0	-
3	32	50	18	40	24.2	0	-
4	32	50	14	40	29.0	13	11.7
5	32	50	10	40	44.3	55	11.7

Table 10.5.1: Varying ambient temperature

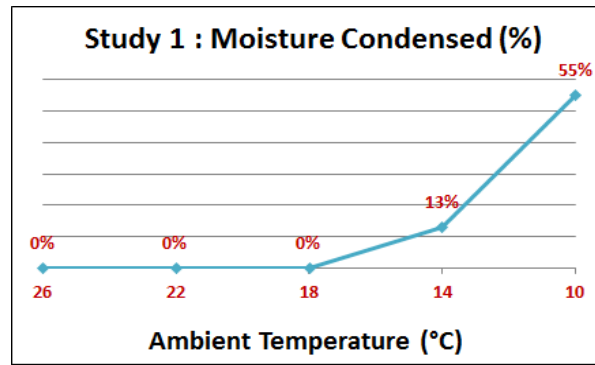


Figure 10.5.4: Varying Ambient Temperature

In study 2, the ambient RH is varied in the range 40-80%, and the RH near the skin is also varied accordingly. The vapour concentration near the skin should be kept higher than the ambient vapor concentration for the mass to be transported in the direction from skin to the film. The difference between the ambient RH and the RH near the skin is maintained at about 10%. Other parameters are kept constant (ambient temperature = 22°C, skin temperature = 32°C). Increasing the ambient RH up to 70% has no effect of condensation. Further increase in the ambient RH shows an effect of condensation. Higher percentage of moisture is condensed with the higher ambient RH. The moisture condensed is about 80% when the ambient RH is kept at 80% (Figure 10.5.5). This is explained with the lower saturation concentration at such high ambient humidities.

S.No	Skin Temperature(°C)	RH near skin (%)	Ambient Temperature(°C)	Ambient RH (%)	EW (g/m ² h)	Moisture condensed (%)	Location of condensation start (mm)
6	32	50	22	40	20.9	0	-
7	32	60	22	50	24.3	0	-
8	32	70	22	60	27.6	0	-
9	32	80	22	70	47.5	54	11.4
10	32	90	22	80	72.6	80	10.7

Table 10.5.2: Varying ambient RH and RH near skin

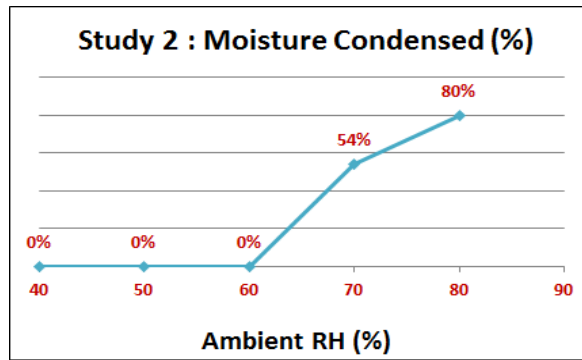


Figure 10.5.5: Varying Ambient RH

In study 3, the skin temperature is varied in the range 28°C to 32°C, the other parameters are kept constant (ambient RH = 40%, ambient temperature = 22°C, RH near skin = 50%). From Figure 10.5.6, it is seen that at the conditions of study 3, varying the skin temperature without varying the ambient conditions does not give any effect on condensation.

S.No	Skin Temperature(°C)	RH near skin (%)	Ambient Temperature(°C)	Ambient RH (%)	EW (g/m ² h)	Moisture condensed (%)	Location of condensation start (mm)
11	36	50	22	40	30.1	0	-
12	34	50	22	40	25.3	0	-
13	32	50	22	40	20.9	0	-
14	30	50	22	40	17.0	0	-
15	28	50	22	40	13.4	0	-

Table 10.5.3: Varying skin temperature

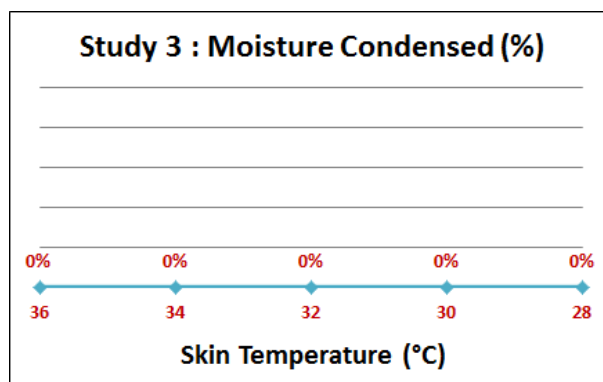


Figure 10.5.6: Varying Skin Temperature

In study 4, the RH near skin is varied from 50% to 90%, keeping the other parameters constant (ambient RH = 40%, ambient temperature = 22°C, skin temperature = 32°C). From Figure 10.5.7, it is seen that with the increase in RH up to the 70%

does not show condensation. The RH increase beyond 70% shows an increase of the percentage of moisture condensed. At the RH near the skin of 90%, the moisture condensed is about 40%. The condensation is explained with the high vapour concentration at the skin, which is higher than the saturation concentration further down in the cooler parts of the porous domain.

S.No	Skin Temperature(°C)	RH near skin (%)	Ambient Temperature(°C)	Ambient RH (%)	EW (g/m ² h)	Moisture condensed (%)	Location of condensation start (mm)
16	32	50	22	40	20.9	0	-
17	32	60	22	40	28.7	0	-
18	32	70	22	40	36.5	0	-
19	32	80	22	40	47.7	10	11.7
20	32	90	22	40	69.9	39	11

Table 10.5.4: Varying the RH near skin

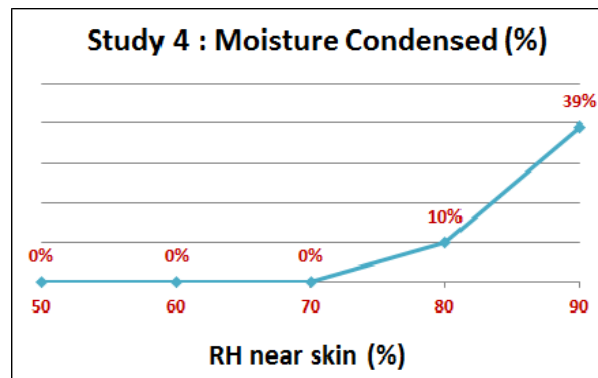


Figure 10.5.7: Varying the RH near skin

In reality, as discussed in literature, temperature and relative humidity are inter-linked. Hence when there is a change with ambient temperature, it is important to have changes in the ambient RH as well. In the coming study, the difference between the ambient RH and the RH near the skin is decided around 5%. Varying a combination of parameters in three different trials is done in the analysis. These trials are decided to be done in order to study the phenomenon of condensation. In trial 1, the skin temperature, the RH near the skin, the ambient temperature and the ambient RH are set to be 32°C, 52%, 20°C, 47% respectively. In trial 2, the skin temperature, the RH near the skin, the ambient temperature and the ambient RH are set to be 32°C, 60%, 18°C, 54% respectively. In trial 3, skin temperature of 32°C, RH near skin of 70%, ambient temperature of 15°C and ambient RH of 65% are set. With trial 3, maximum amount of condensation is seen to be achieved and the percentage of moisture condensed is about 75% (see Figure 10.5.8). Since the condensation effect is highly pronounced in this trial, it is taken as a relevant case in the following study to check for the other factors affecting condensation. The temperature and the RH could be varied in the future studies, also the consideration of specific differences between the skin RH and the ambient RH could be eliminated.

S.No	Skin Temperature($^{\circ}\text{C}$)	RH near skin (%)	Ambient Temperature($^{\circ}\text{C}$)	Ambient RH (%)	EW ($\text{g}/\text{m}^2\text{h}$)	Moisture condensed (%)	Location of condensation start (mm)
21	32	52	20	47	21.5	0	-
22	32	60	18	54	29.9	15	11.7
23	32	70	15	65	67.0	75	11.1

Table 10.5.5: Varying Ambient Temperature, Ambient RH and the RH near the skin

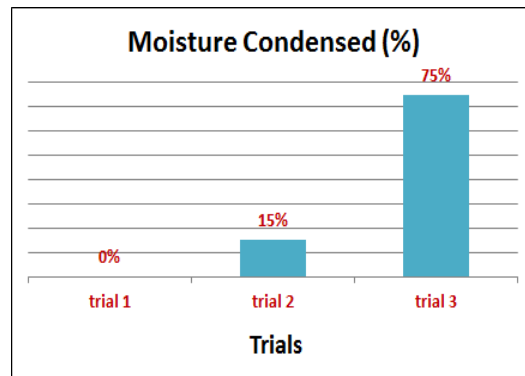


Figure 10.5.8: Varying Ambient Temperature, Ambient RH and the RH near the skin

10.5.2 Significance of Condensation

The stated conditions in trial 3 are incorporated in the model and condensation is seen to start near the end of the porous domain where the vapour concentration is higher than the saturation concentration (Figure 10.5.9). With condensation, location of the start of the phenomena has also been observed and it has been inferred that in all the simulations dealt until now, the percentage of moisture condensed is related to the onset of condensation within the porous domain. Higher the percentage of moisture condensed, onset of condensation is further away from the inner boundary of the porous medium.

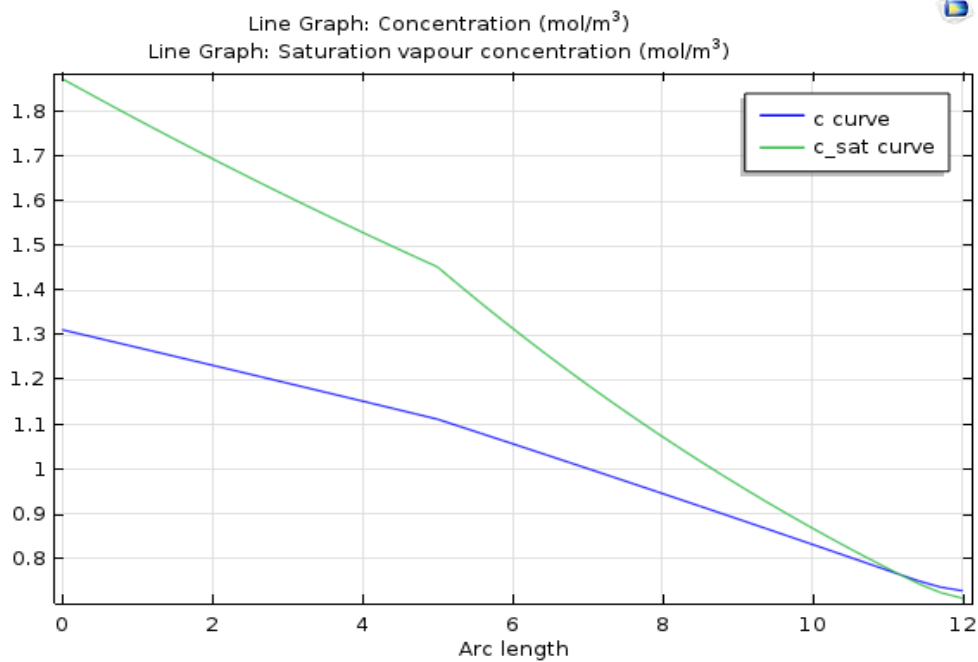


Figure 10.5.9: Trial 3 - c and c_{sat} curve comparison

Two cut line 1D plots for the study of the same case with and without condensation are created within the same graph for the variables temperature and concentration (Figure 10.5.10 and Figure 10.5.11). With condensation included in the model, there are changes in the temperature and concentration curves, and also changes in the heat flux and the mass flux. This is explained with the energy transfer happening from gas to liquid phase and the accumulation of liquid droplets on the surface respectively. With the effect of condensation, it is interesting to notice the slight increase of about 3% in the normal boundary conductive heat flux at the skin and at the inner boundary of the porous domain but a huge decrease of about 65% at the film. This behaviour with the model is explained with the effect of condensation when the energy is being transferred from vapour to liquid phase, less energy is available to be transported giving reason to the low conductive flux at the film. With the mass transport, there is a huge increase of about 97% in the normal boundary diffusive flux at the skin and at the inner boundary of the porous domain, and a decrease of 51% in the diffusive flux at the film.

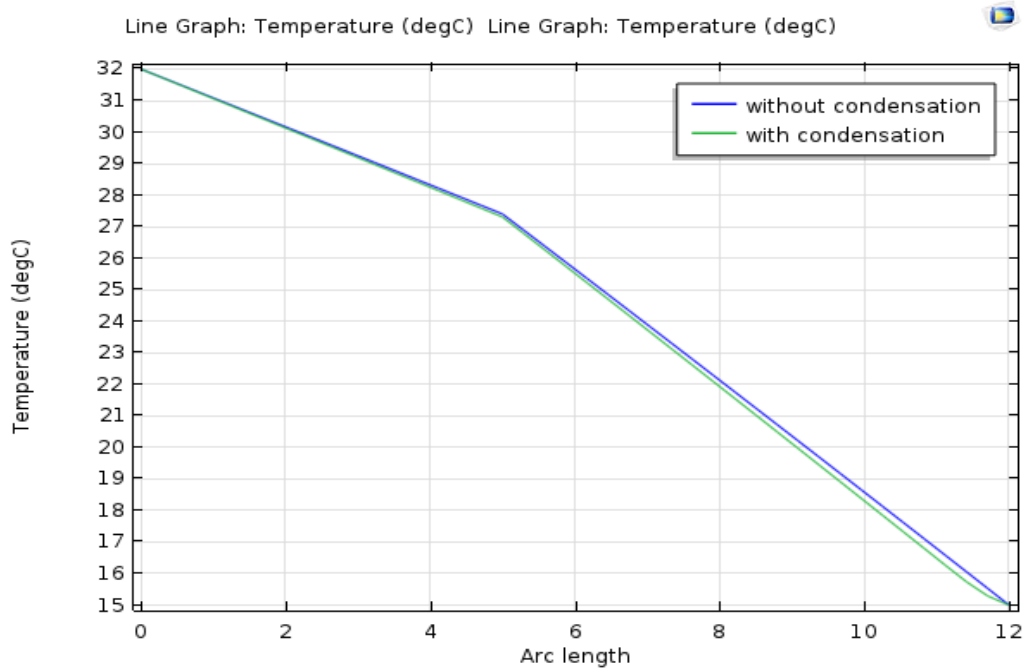


Figure 10.5.10: Trial 3 - Temperature curve

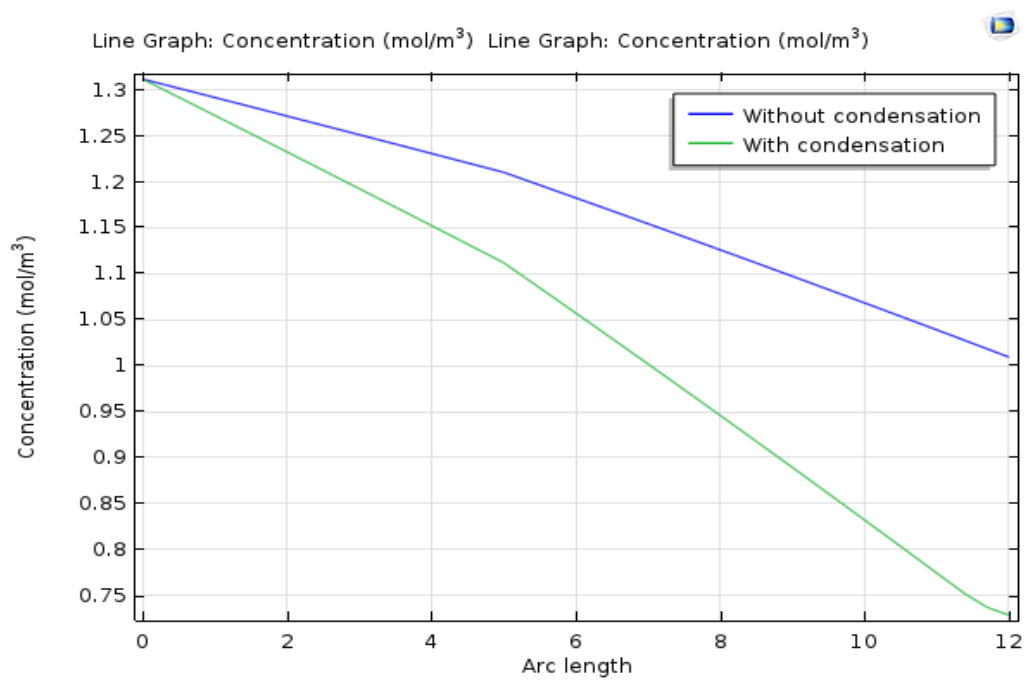


Figure 10.5.11: Trial 3 - Concentration curve

As it is evident that condensation has its effect on the heat and the mass transfer processes, it is significant to be included in the model.

10.5.3 Effect of evaporated water(EW)

It is interesting to check the effect of condensation when the difference between the RH near skin and the ambient RH is higher. The ambient conditions are kept the same as in Trial 3, and the RH near the skin is increased. It is seen that a higher difference in the RH gave higher EW values, for example, the case with the EW 110 g/m²h, which is higher than the regular TEWL range. A higher percentage of moisture is condensed when the EW is higher.

In this study case, the location of condensation has been observed. Condensation starts at 10 mm and 11.1 mm for a higher EW case and lower EW case respectively, as shown in Table 10.5.6. It is evident in this scenario as well that the condensation starts early within the porous domain with the higher percentage of moisture condensed if the condensation rate is maintained.

S.No	Skin Temperature(°C)	RH near skin (%)	Ambient Temperature(°C)	Ambient RH (%)	EW (g/m ² h)	Moisture condensed (%)	Location of condensation start (mm)
24	32	70	15	65	67	75	11.1
25	32	85	15	65	110	86	10

Table 10.5.6: Varying effect of EW

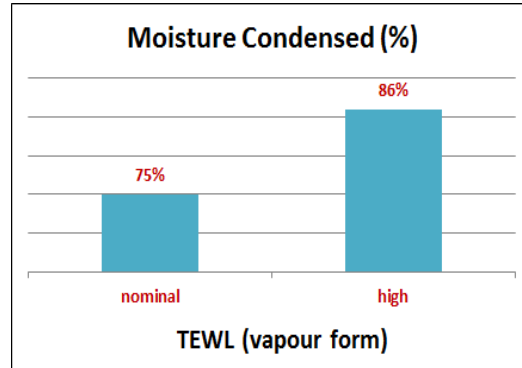


Figure 10.5.12: Varying EW

10.5.4 Effect of Condensation rate

Condensation rate(k) is varied to unrealistic values to understand the condensation trends. This is an advantage of the modelling processes, where the model allows the user to keep the condensation rate as a variable in the initial study and later could be used to predict the rates in reality. Two cases have been analysed where in both of the cases, the condensation rate is varied in the range 0.1 s⁻¹ to 1000 s⁻¹.

- Case 1: skin temperature = 32°C, RH near skin = 50%, ambient temperature = 22°C and ambient RH = 40%

- Case 2: skin temperature = 32°C, RH near skin = 70%, ambient temperature = 15°C and ambient RH = 65%

From figure Figure 10.5.13, it is evident that there is no condensation happening with the case 1 even at a very low or high condensation rate. For the case 2, there are pronounced effects of a very high and a very low condensation rate (Figure 10.5.14). With the higher condensation rate, the percentage of moisture condensed is higher. The condensed amount can go as high as about 77% in the model. When the condensation rates are varied, location of the onset of condensation can be different with the varied amount of moisture condensed. With k as 0.1 s^{-1} , condensation start at 7.6 mm and with k as 10 s^{-1} , condensation starts at around 10 mm. The former has about 12% moisture condensed and the latter has about 70% moisture condensed. The higher the condensation rate, the higher is the percentage of moisture condensed implying that the onset of condensation is late within the porous domain. This clearly shows that the relation of the percentage of moisture condensed with the onset of condensation is the opposite if the condensation rates are varied.

S.No	Condensation rate (s^{-1})	EW ($\text{g}/\text{m}^2\text{h}$)	Moisture condensed (%)	Location of the condensation start (mm)
26	0.1	20.9	0	-
27	10	20.9	0	-
28	100	20.9	0	-
29	500	20.9	0	-
30	1000	20.9	0	-

Table 10.5.7: Varying Condensation rate with Case 1

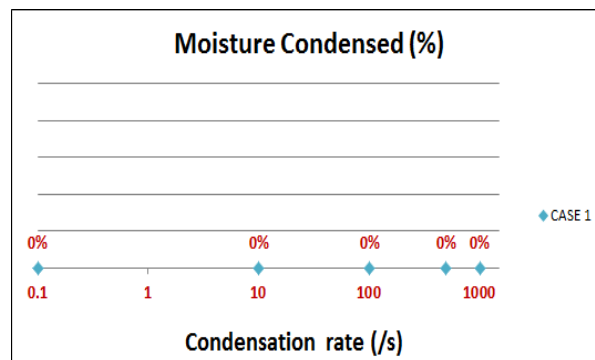


Figure 10.5.13: Varying Condensation rate with Case 1

S.No	Condensation rate (s^{-1})	EW (g/m^2h)	Moisture condensed (%)	Location of the condensation start (mm)
31	0.1	37.0	12	7.6
32	10	64.0	70	10.0
33	100	67.0	75	11.1
34	500	67.3	76	11.7
35	1000	67.3	77	11.7

Table 10.5.8: Varying Condensation rate with Case 2

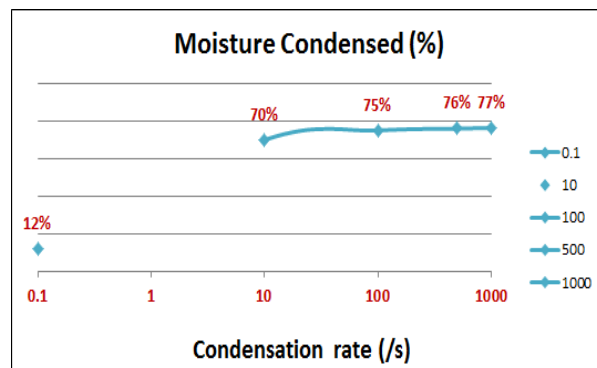


Figure 10.5.14: Varying Condensation rate with Case 2

10.5.5 Thickness of porous domain

The objective of this section is to check the effect of condensation with respect to the thickness of the porous domain. From the Figure 10.5.15, it is inferred that with higher thickness, there is a lower percentage of moisture condensed. This is explained by the diffusion path being higher in the model with higher porous domain thickness. Thickness does not seem to affect the onset of condensation. Irrespective of the varied thickness, the condensation starts around the end of the porous domain because of the lower temperature at that site. With 3 mm and 10 mm thick porous domain, the moisture condensed is 83% and 69% respectively.

S.No	Thickness of porous domain (mm)	EW (g/m^2h)	Moisture condensed (%)	Location of the condensation start (mm)
36	3	105	83	7.4
37	5	82.0	79	9.1
38	7	67.0	75	11.1
39	10	52.4	69	14.1

Table 10.5.9: Varying porous domain thickness

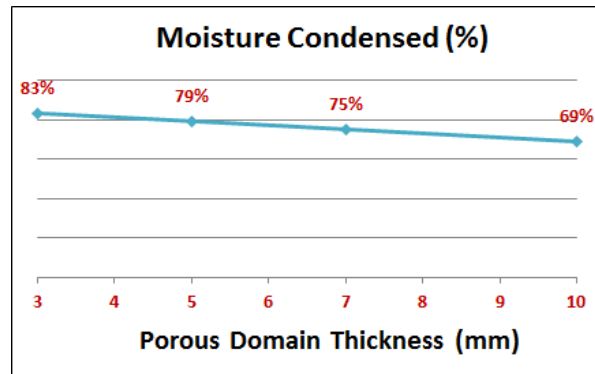


Figure 10.5.15: Varying porous domain thickness

10.5.6 Thickness of the air layer

The study model in the analysis has eliminated the effect of convection since the air layer in the pre-study is kept at 5 mm. Through the use of dimensionless numbers, the air layer of 5 mm thickness did not prove high enough effect for convection to be included. Hence if the thickness is to be varied, there is a limit to the maximum thickness allowed in this study model and it is to be estimated with the changing model inputs. In this analysis, the range of air layer thickness is 3 mm to 6 mm, which is in the safe range of neglecting convection. From Figure 10.5.16, it is inferred that with the increase in air layer thickness, the percentage of moisture condensed decreases. The reason behind this could be the same as with the effect of porous domain thickness, that is, the diffusion path is increased. The location of the start of condensation is not affected much with the varied thickness and is witnessed near the end of the porous domain.

S.No	Air Layer Thickness (mm)	EW (g/m ² h)	Moisture condensed (%)	Location of the condensation start (mm)
40	3	78.3	79	9.1
41	5	67.0	75	11.1
42	6	62.3	73	12.1

Table 10.5.10: Varying air layer thickness

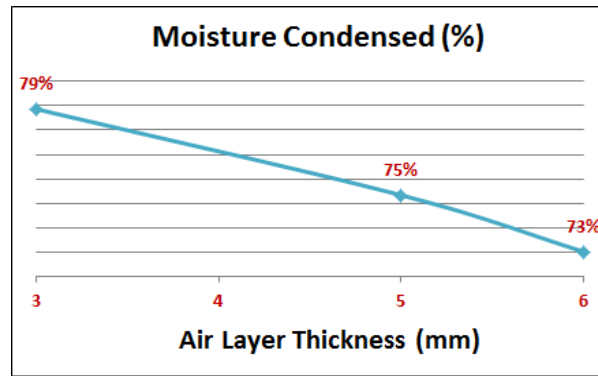


Figure 10.5.16: Varying air layer thickness

10.5.7 Porosity of the porous domain

The porosity of the porous domain has been varied in the range 0.7 to 0.9 and the effect of condensation is checked. With the higher porosity, the higher the percentage of moisture condensed (Figure 10.5.17). At a porosity of 0.7, the amount condensed is 72% and at a porosity of 0.9, it is 78%. Higher porosity for heat transport processes resulting in larger percentage of moisture being condensed. But it is interesting to see that the difference in the amount condensed with the varying porosity is not varying much.

S.No	Porosity of porous domain core	EW (g/m ² h)	Moisture condensed (%)	Location of the condensation start (mm)
43	0.7	59.1	72	11.1
44	0.8	67.0	75	11.1
45	0.9	74.1	78	11.1

Table 10.5.11: Varying porosity of the porous domain

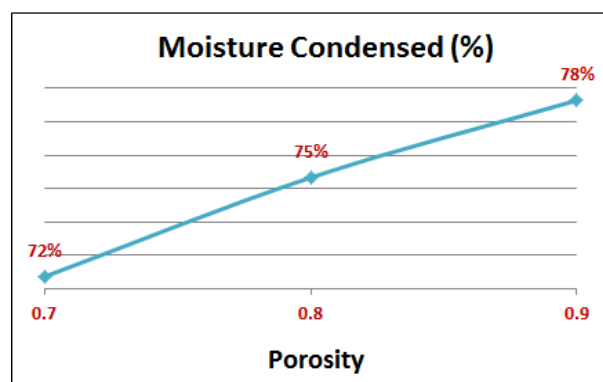


Figure 10.5.17: Varying porosity of the porous domain

10.5.8 Breathability of the film

Effect of condensation has been investigated for non-breathable and high breathable films. The former having Mocon number of 55 g/m²24h and the latter having Mocon numbers of 5000 g/m²24h and 7000 g/m²24h. From the Figure 10.5.18, it is understood that the higher the breathability, the lower is the risk of condensation. With the non-breathable film, condensation is shown to be maximum. This is explained with the restriction to limit the moisture that could be escaped from the non-breathable film. Such restriction is bound to contain the entire moisture within the system, which eventually get condensed as liquid droplets on the surface.

S.No	Breathability of backsheet (g/m ² 24h)	EW (g/m ² h)	Moisture condensed (%)	Location of the condensation start (mm)
46	55	67.4	100	11.1
47	5000	67.0	75	11.1
48	7000	66.4	65	11.1

Table 10.5.12: Varying film breathability

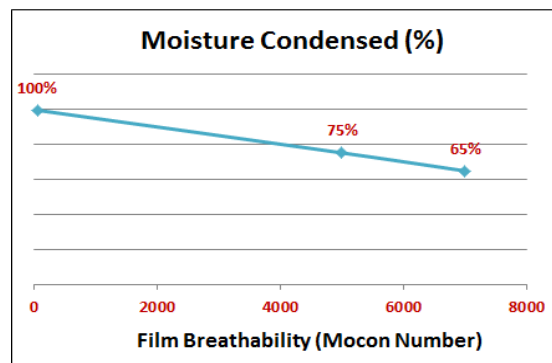


Figure 10.5.18: Varying film breathability

11

Conclusion

11.1 Skin Model

Though the bodily mechanisms are not accounted for, a realistic way can be seen to define the body at steady state as a surface with certain temperature emitting certain moisture outward. The temperature at the skin surface could be in the range 28°C to 35°C. The RH near the skin has been difficult to predict. Hence as mentioned before it is estimated by means of a sub model using constant skin diffusive flux and skin temperature as inputs. From the literature reading, there has been a case where TEWL is measured when the skin is not occluded by any material, which is used to decide the EW range in the sub model. The range of EW is decided to be slightly broader as the skin in the model is occluded with some material. Then, the estimation of the RH near the skin is carried out, as shown in (Table 11.1.1). It is concluded that the RH near skin is dependent on the ambient and skin temperature, EW and the ambient RH.

Skin Temperature (°C)	Ambient Temperature (°C)	Ambient RH (%)	Range of RH near skin (%)	EW range (g/m ² h)
32	22	40	50-70	20.9-37

Table 11.1.1: Estimation of RH near skin

11.2 Heat and Mass Transport

Due to the higher skin surface temperature and skin surface concentration when compared to the ambient temperature and ambient concentration, the direction of heat and mass transfer is from skin towards the film. There is more resistances for the heat and mass in the porous domain leading to different temperature and concentration gradients in the two domains.

Due to the negligible pressure differences and the low flow due to gravity, the driving forces for the flow are not strong enough for the flow to be accounted in the model.

Using the Rayleigh number, the transport due to flow can be shown to be negligible in comparison to transport due to conduction. Accordingly the flow component is neglected in the model.

Effect of radiation

The body emits around $492\text{W}/\text{m}^2$, being a major source of radiation in the model. The total flux emitted from the skin surface is higher than the flux emitted from the inner boundary of the porous domain. This results in a net radiative flux from skin towards the porous domain. Including radiation in the model results in an increase in temperature of about 2°C at the inner layer of the porous medium. The temperature rise accounts for 20% of the temperature difference considered in the model, and hence radiation has to be included in the study.

11.3 Condensation

Condensation happens when the vapour concentration is greater than the saturation vapour concentration. The excess vapour is condensed as liquid on the surface, for example, on the solid surface inside the porous medium. Due to condensation, heat loss and the moisture loss are seen in the vapour phase. Hence the heat sink and the mass sink terms are added to the heat transfer and mass transfer equations respectively to account for the heat losses and the mass losses. The effect of condensation in the model is checked by visualizing the vapour concentration and saturation vapour concentration curves. The point of intersection of the vapour concentration and the saturation vapour concentration is the location of the start of condensation within the porous medium. The location is calculated in the simulation model. The percentage of moisture condensed is estimated from the diffusive flux at the skin and the diffusive flux at the film boundary.

There is decrease in temperature and concentration curves with the effect of condensation and also changes in the heat flux and the mass flux.

Influence of various parameters

Condensation is highly prevalent due to certain ambient conditions, which influence the rate of condensation.

After a set of few simulations, there has been trends identified for the parameters - porous medium thickness, air layer thickness, porosity of the porous medium and breathability of the film. The following have been identified :

- The higher the porous medium thickness, the lower the percentage of moisture condensed
- The lower the air layer thickness, the higher the percentage of moisture condensed
- The lower the porosity of the porous medium, the lower the percentage of moisture condensed. The difference with the effect of varying porosity is not

high when compared to other parameters.

- The higher the breathability of the film, the lower the percentage of moisture condensed

11. Conclusion

12

Future Research

Some future works can be done using the current model as a base of modelling and analysis.

- The risk of condensation in the model is visualized for the cases where the vapour concentration gets higher than the saturation vapour concentration, that is the case when the relative humidity becomes greater than 100%. There are cases where condensation is bound to happen when the relative humidity is lesser than 100% as well, which is the case with capillary condensation. Since capillary condensation is dependent on the pore geometry, microstructure model for the porous medium has to be investigated to analyse the effect of capillary condensation.
- The model in this study is restricted to stagnant air conditions. It is interesting to see the effect of wind speed with the heat and mass transfer processes and as well with the condensation within the porous medium. To include this, convection and advection have to be included to the base model after analyzing the proper boundary conditions to represent them in COMSOL.
- The model in this study deals with steady state analysis. A transient study could be useful to visualise the effect of condensation with time. It gives a path to incorporate absorption in the model to understand the effect of the phenomenon.
- The porous medium in the model is restricted to be a cellulose fibre layer. This layer could be replaced with another potential material layer to visualise and compare its influence with the cellulose fibre. Alternatively, successive layers could be added in addition to the cellulose fibre layer to check for the effect of combination of materials in the porous medium.
- The project aim is limited to the vapour phase transport. An interesting study is to consider the wet diaper which would involve the liquid phase transport in addition in the model.

Bibliography

- [1] Huaxiong Huang, Changhua Ye, and Weiwei Sun Huan. Moisture transport in fibrous clothing assemblies. *J Eng Math*, 61:35–54, 2008.
- [2] Yunyi Wang, Ziwei Huang, Yehu Lu, Mengmeng Zhao, and Jun Li. Heat transfer properties of the numerical human body simulated from the thermal manikin. *The Journal of The Textile Institute*, 102(2):178–187, 2012.
- [3] D. Soulat E. Onofrei. Modeling of heat transfer through multilayer firefighter protective clothing. 65(5):277–283, 2014.
- [4] Van De Linde F. Lotens, W. and G. Havenith. Effects of condensation in clothing on heat transfer. *Ergonomics*, 38(6):1114–1131, 1995.
- [5] A. (n.d.) Rasmuson. *Mathematical modeling in chemical engineering*. Cambridge University Press, 2014.
- [6] Sca at a glance.
- [7] Sca personal care at a glance.
- [8] C. White. Engineered structures for use in disposable incontinence products. *Journal of Engineering in Medicine*, 217(4):243–251, 2003.
- [9] Castellani V. Mirabella, N. and S. Sala. Life cycle assessment of bio-based products: a disposable diaper case study. *Int J Life Cycle Assess*, 18(5):1036–1047, 2013.
- [10] Schlatter H. Ochsenhirt J. Krause E. Marsman D. Kosemund, K. and G. Erasala. Safety evaluation of superabsorbent baby diapers. *Regulatory Toxicology and Pharmacology*, 53(2):81–89, 2009.
- [11] Helmes C. White J. Dey, S. and S. Zhou. Safety of disposable diaper materials: Extensive evaluations validate use. *Clinical Pediatrics*, 53(9S):17S–19S, 2014.
- [12] Lund K. Brelid H. Brodin, F. and H. Theliander. Reinforced absorbent material: a cellulosic composite of tempo-oxidized mfc and ctmp fibres. *Cellulose*, 19(4):1413–1423, 2012.
- [13] Chandrashekhhar Malviya and Anjani K. Dwivedi. Studies on convective heat transfer in porous media. *Journal of Industrial Pollution Control*, 2012.

- [14] F.A.L. Dullien. *Porous media: Fluid transport and pore structure*. Academic Press, 1992.
- [15] Audra Wright and Frank Akin. Comfort perception of breathable and non-breathable diapers. 2005.
- [16] Chris Shelley Bert Woelfli P.C. Wu, Greg Jones. Novel microporous films and their composites. *Journal of Engineered Fibers and Fabrics*, 2(1), 2007.
- [17] *Skin structure and function*. Washington.
- [18] D. Voegeli. Moisture-associated skin damage: an overview for community nurses. *Br J Community Nursing*, 18(1):6–12, 2013.
- [19] Howard I Maibach Steven B.Hoath. *Neonatal Skin: Structure and Function*. CRC Press, 2003.
- [20] P. Agache and P. Humbert. *Measuring the skin*. Springer, Berlin, 2004.
- [21] Jemec G. Serup, J. and G. Grove. *Handbook of non-invasive methods and the skin*. CRC/Taylor Francis, Boca Raton, 2006.
- [22] B. Andersson. *Computational Fluid Dynamics for Engineers*. Cambridge University Press, Cambridge, 2015.
- [23] What are the navier-stokes equations?. [accessed 15 jun. 2016].
- [24] C. Ho and S. Webb. *Gas transport in porous media*. Springer, Dordrecht, 2006.
- [25] *Private discussion with Charlotta Hanson*. SCA, March 2016.
- [26] D. Nield and A. Bejan. *Convection in porous media*. Springer, New York, 2013.
- [27] Wilson R.E. Welty J.R., Wicks C.E. and Rorrer G. *Fundamentals of Momentum, Heat, and Mass Transfer, 5th Edition*. John Wiley Son, New York, 2007.
- [28] Y.A. Cengel. *Introduction to Thermodynamics and Heat Transfer*. McGraw-Hill, New York, 1997.
- [29] R. Siegel and J. Howell. *Thermal radiation heat transfer*. CRC Press.
- [30] *Private discussion with Anders Rasmuson*. Chalmers University of Technology, March 18,2016.
- [31] V.K.Kothari R.Fanguiero Brojeswari Das, A.Das and M. de Araújo. Moisture transmission through textiles, Part I: Processes involved in moisture transmission and the factors at play. *AUTEX Research Journal*, 7(2), 2007.
- [32] Ag.auburn.edu.[accessed 26 may 2016].
- [33] P. Wahlgren. *Convection in Loose-fill Attic Insulation*. Chalmers University of Technology. (PhD Thesis, Department of Building Physics), Göteborg, 2001.

-
- [34] M. Glomski and M.A. Johnson. A precise calculation of the critical rayleigh number and wave number for the rigid-free rayleigh-benard problem. *Applied Mathematical Sciences*, 103(6):5097–5108, 2012.
- [35] Y. Shiina and M. Hishida. Critical rayleigh number of natural convection in high porosity anisotropic horizontal porous layers. *International Journal of Heat and Mass Transfer*, 53(7):1507–1513, 2010.
- [36] J. (n.d). Kuneš. *Dimensionless physical quantities in science and engineering*. 2012.
- [37] C. Wen. *The fundamentals of aerosol dynamics*. World Scientific, Singapore, 1996.
- [38] Comsol multiphysics modeling software.
- [39] Y. Li and B Holcombe. Mathematical simulation of heat and moisture transfer in a human-clothing-environment system. *Textile Research Journal*, 68(6):389–397, 1998.
- [40] Ghaddar N. Salloum, M. and K. Ghali. A new transient bioheat model of the human body and its integration to clothing models. *International Journal of Thermal Sciences*, 46(4):371–384, 2007.
- [41] Li B. Zhang, Q. and W. Sun. Heat and sweat transport through clothing assemblies with phase changes, condensation/evaporation and absorption. *Proceedings of the Royal Society A: Mathematical, Physical and Engineering Sciences*, pages 3469–3489, 2011.
- [42] Meinander H. Celcar, D. and J. Geršak. A study of the influence of different clothing materials on heat and moisture transmission through clothing materials, evaluated using a sweating cylinder. *International Journal of Clothing Science and Technology*, 20(2):119–130, 2008.
- [43] H. Meinander. Clothing physiological measurements on winter workwear materials with a sweating cylinder. *The Journal of The Textile Institute*, 79(4):620–633, 1988.
- [44] Venditti R. Rojas O. Habibi Y. Spence, K. and J. Pawlak. A comparative study of energy consumption and physical properties of microfibrillated cellulose produced by different processing methods. *Cellulose*, 18(4):1097–1111, 2011.
- [45] Goodfellow - catalogue. [accessed 15 jun. 2016].
- [46] Gellert R. Spitzner M. Pfundstein, M. and A.G Rudolphi. *Insulating Materials*. DETAIL - Institut fur internationale Architektur-Dokumentation GmbH Co. KG, Munchne, 2008.
- [47] S. Mortstedt and G Hellsten. *Data och diagram*. Liber utbildning, Stockholm, 1994.

- [48] Thermal conductivity of some common materials and gases. [accessed 15 jun. 2016].
- [49] Table of emissivity in the ir spectrum. [accessed 15 jun. 2016].
- [50] *Heat Transfer Module User's Guide 5.2*. Comsol Multiphysics, 2016.
- [51] Tupkek R. Agner T. Pinnagoda, J. and J. Serup. Guidelines for transepidermal water loss (tewl) measurement. *Contact Dermatitis*, 22(3):164–178, 1990.
- [52] Audra Wright and Frank Akin. Comfort perception of breathable and non-breathable diapers. *Kimberly-Clark Corporation*, 2005.

A

Appendix

A.1 Calculations

Concentration calculation with known RH

Step 1: Calculation of Partial vapor pressure P_a (unit in Pascals). Saturation vapor pressure P_s is found from COMSOL.

$$\frac{RH(\%)}{100} = \frac{P_a}{P_s}$$

Step 2: Calculation of the concentration of the vapor (unit in mol/m³)

$$P_a V = nRT$$

$$\frac{n}{V} = \frac{P_a}{RT}$$

Diffusion Coefficient

A denotes air and B denotes water vapor,

$$D_{AB} = \frac{10^{-3} T^{1.75} \left(\frac{1}{M_A} + \frac{1}{M_B} \right)^{\frac{1}{2}}}{P \left[(\Sigma v)_A^{\frac{1}{3}} + (\Sigma v)_B^{\frac{1}{3}} \right]^2}$$

$$\Rightarrow D_{AB} = \frac{10^{-3} T^{1.75} \left(\frac{1}{28.97} + \frac{1}{18.01} \right)^{\frac{1}{2}}}{1 \left[(19.7)^{\frac{1}{3}} + (11.6)^{\frac{1}{3}} \right]^2}$$

$$\Rightarrow D_{AB} = 1.175 \cdot 10^{-5} T^{1.75} \text{ cm}^2/\text{s}$$

Where D_{AB} is in cm²/s, T is in Kelvin, P is in atm.

Diffusion calculated from the Mocon number

$$\text{Mocon number} = 5000 \text{ g/m}^2 \text{ 24h} \Rightarrow 3.22 \cdot 10^{-3} \text{ mol/m}^2\text{s}$$

$$N = -\frac{D_b}{d_s}(C_{amb} - c)$$

Where d_s and D_b denotes the thickness of the back sheet and diffusion coefficient of water vapour through the back sheet respectively. C_{amb} is the ambient concentration; c is the concentration(mass transport dependent variable).

$$d_s = 18 \cdot 10^{-6} \text{ m}$$

$$N = 3.22 \cdot 10^{-3} \text{ mol/m}^2\text{s}$$

$$D_b = 2.22 \cdot 10^{-4} \text{ cm}^2/\text{s}$$

$$D_{air} = 0.300643 \text{ cm}^2/\text{s}$$

$$\text{Assumption} \Rightarrow C_{amb} - c = 2.61 \text{ mol/m}^3$$

After substitution,

$$D_b = \mathbf{0.00073} D_{air}$$

$$\text{Porosity of the film} = 0.00073$$

A.2 Boundary Conditions



Figure A.2.1: Temperature(ht),
Concentration(tds)



Figure A.2.2: Heat Flux(ht),
Flux(tds)



Figure A.2.3: Symmetry(ht,tds)



Figure A.2.4: Diffuse Surface(ht)

Module

ht - Heat Transfer for Porous Media

tds- Transport of Diluted Species

B

Appendix

B.1 Results

Heat Transport

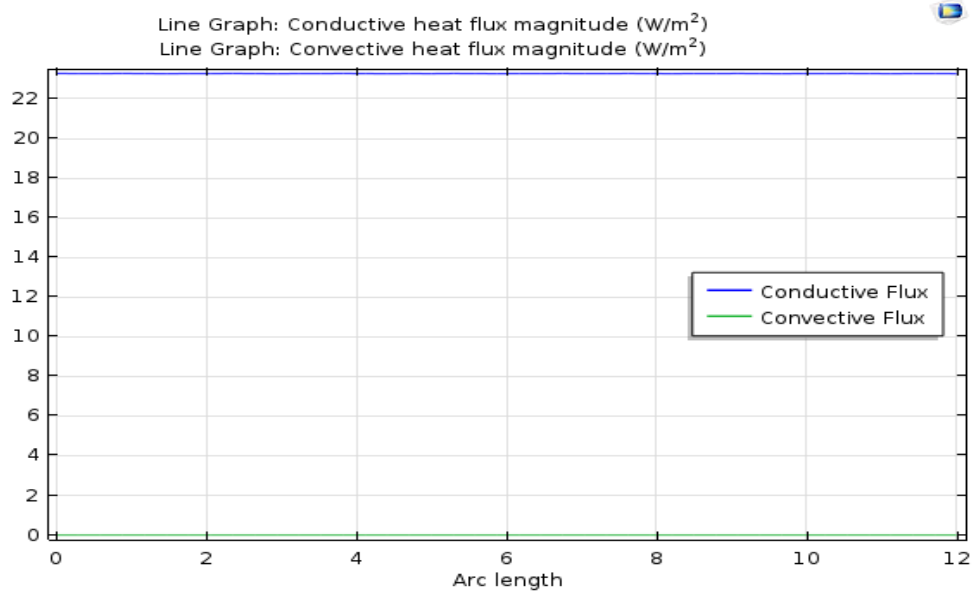


Figure B.1.1: Heat Flux within the model

Mass Transport

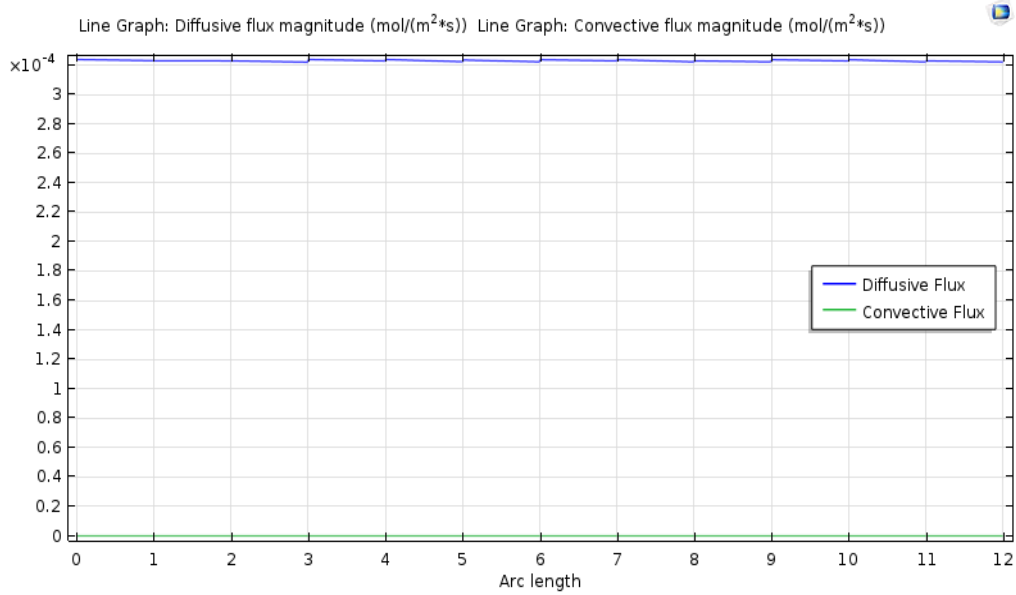


Figure B.1.2: Mass Flux within the model

Effect of Radiation

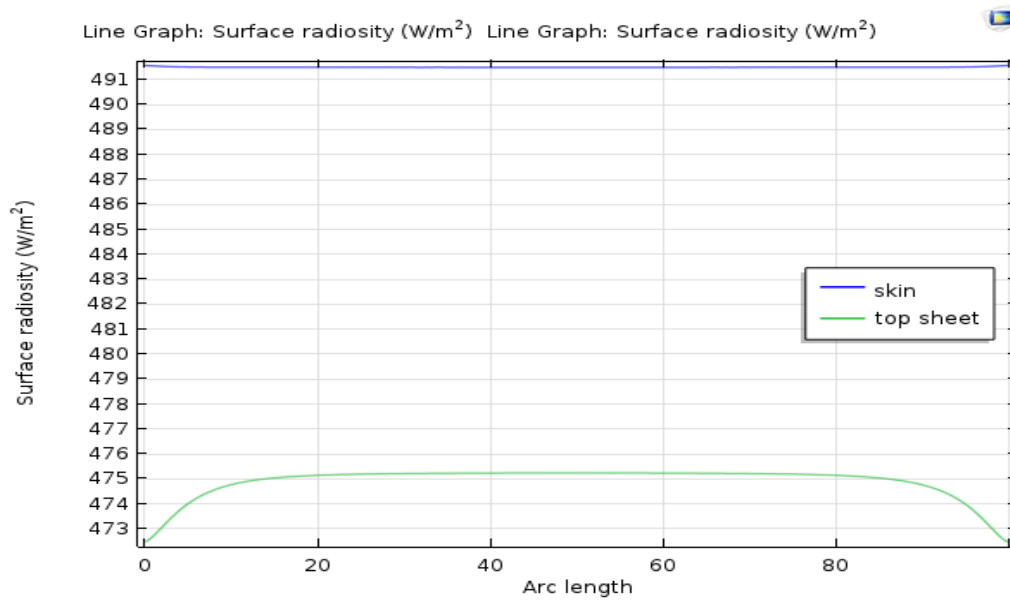


Figure B.1.3: Surface Radiosity